

Developing Future Projected Intensity-Duration-Frequency (IDF) Curves

A Technical Report on Data, Methods, and IDF Curves for the Chesapeake Bay Watershed and Virginia

MICHELLE E. MIRO, ARTHUR T. DEGAETANO, TANIA LÓPEZ-CANTÚ,
CONSTANTINE SAMARAS, MARISSA WEBBER,
KRISTA ROMITA GROCHOLSKI

Sponsored by Chesapeake Bay Trust



RAND SOCIAL AND ECONOMIC WELL-BEING

For more information on this publication, visit www.rand.org/t/TLA1365-1.

About RAND

The RAND Corporation is a research organization that develops solutions to public policy challenges to help make communities throughout the world safer and more secure, healthier and more prosperous. RAND is nonprofit, nonpartisan, and committed to the public interest. To learn more about RAND, visit www.rand.org.

Research Integrity

Our mission to help improve policy and decisionmaking through research and analysis is enabled through our core values of quality and objectivity and our unwavering commitment to the highest level of integrity and ethical behavior. To help ensure our research and analysis are rigorous, objective, and nonpartisan, we subject our research publications to a robust and exacting quality-assurance process; avoid both the appearance and reality of financial and other conflicts of interest through staff training, project screening, and a policy of mandatory disclosure; and pursue transparency in our research engagements through our commitment to the open publication of our research findings and recommendations, disclosure of the source of funding of published research, and policies to ensure intellectual independence. For more information, visit www.rand.org/about/principles.

RAND's publications do not necessarily reflect the opinions of its research clients and sponsors.

Published by the RAND Corporation, Santa Monica, Calif.

© 2021 RAND Corporation

RAND® is a registered trademark.

Limited Print and Electronic Distribution Rights

This document and trademark(s) contained herein are protected by law. This representation of RAND intellectual property is provided for noncommercial use only. Unauthorized posting of this publication online is prohibited. Permission is given to duplicate this document for personal use only, as long as it is unaltered and complete. Permission is required from RAND to reproduce, or reuse in another form, any of its research documents for commercial use. For information on reprint and linking permissions, please visit www.rand.org/pubs/permissions.

Preface

This report describes the motivation, data, methods and results from a cross-institutional research project to generate future projected intensity-duration-frequency (IDF) curves for both the Chesapeake Bay Watershed and the Commonwealth of Virginia. As a technical report, it will complement other key outcomes of this project—an online interactive tool with the final study results, an online webinar to walk users and interested parties through methods and the tool, and a series of academic journal articles that highlight the scientific contributions of this effort and put this work in the context of scientific research. The scope of this study was centered around the production of future projected IDF curves and ensuring that they were accessible online and based on transparent methods. Therefore, we did not include a deep academic-style literature review in this report and focused instead on the technical details, noting relevant peer-reviewed literature that underpins the methods. The aim of this report is to make the project’s data and methodology clear and transparent to those using the interactive online IDF curve tool or those interested in replicating these methods in other contexts. The IDF curve tool is available at <https://midatlantic-idf.rcc-acis.org>.¹

This project was carried out by researchers at Carnegie Mellon University (CMU), the Northeast Regional Climate Center (NRCC) at Cornell University, and the RAND Corporation. The project team members from RAND and the NRCC are also a part of the Mid-Atlantic Regional Integrated Sciences and Assessments (MARISA) program, described below. Within RAND, this project resides in the Community Health and Environmental Policy Program.

The project was funded by the Chesapeake Bay Trust under the Chesapeake Bay Program’s Goal Implementation Team to develop future projected IDF curves for locations within the bounds of the Chesapeake Bay Watershed. The NRCC and CMU also received funding from the Virginia Transportation Research Council and the Commonwealth Center for Recurrent Flooding Resiliency to extend the study boundaries to include the full state of Virginia.

Mid-Atlantic Regional Integrated Sciences and Assessments Program

The MARISA program was established in September 2016 with a five-year grant from the National Oceanic and Atmospheric Administration (NOAA). It is one of 11 RISA programs across the United States and Pacific Islands funded by the NOAA Climate Program Office. MARISA supports integrated, flexible processes for building adaptive capacity to climate variability and change in diverse settings in the mid-Atlantic region, with an initial focus on the Chesapeake Bay Watershed. MARISA is led by the RAND Corporation, in partnership with researchers in the Earth and Environmental Systems Institute at the Pennsylvania State

¹ Mid-Atlantic Regional Integrated Sciences and Assessments, “Projected Intensity-Duration-Frequency (IDF) Curve Data Tool for the Chesapeake Bay Watershed and Virginia,” undated.

University and the Environment, Energy, Sustainability and Health Institute at Johns Hopkins University, along with support from researchers at the NRCC at Cornell University and the Virginia Institute of Marine Science.

Community Health and Environmental Policy Program

RAND Social and Economic Well-Being is a division of the RAND Corporation that seeks to actively improve the health and social and economic well-being of populations and communities throughout the world. This research was conducted in the Community Health and Environmental Policy Program within RAND Social and Economic Well-Being. The program focuses on such topics as infrastructure, science and technology, community design, community health promotion, migration and population dynamics, transportation, energy, and climate and the environment, as well as other policy concerns that are influenced by the natural and built environment, technology, and community organizations and institutions that affect well-being. For more information, email chep@rand.org.

The Northeast Regional Climate Center

Housed at Cornell University since 1983, the NRCC is one of six federally supported centers established to meet regional needs for climate data products, research-based information, and climate expertise. NRCC users include businesses; federal, state, and local governments; the media; and private citizens. The NRCC provides climate information to users faced with responding to climate extremes, maximizing economic gains through enhanced agricultural yields, optimizing energy usage, designing infrastructure, and protecting the environment. Through experience, the NRCC has learned that effective climate services require one-on-one interaction with stakeholders both to learn user needs and to develop products that are relevant, usable, and up to date. Users typically require products and information that are dynamic, necessitating that new data be continually collected and incorporated into databases and products. The NRCC and Regional Climate Center (RCC) program are at the forefront of developing operational data support systems. The Applied Climate Information System is the foundation of RCC data management and electronic information delivery. Its flexible modular design allows the NRCC to respond quickly and efficiently to requests for new products and services.

Abstract

The Chesapeake Bay Watershed (CBW) and Virginia have experienced increases in extreme rainfall events over the past few decades, exacerbating stormwater challenges throughout the region. To support the region in mitigating these challenges, this study developed projected intensity-duration-frequency (IDF) curves that can be easily integrated and used across the CBW and Virginia to plan, design, and build infrastructure assets to be more resilient to climate change. The authors leveraged the best-available science to inform and carry out a transparent, consistent, and straightforward approach to generating IDF curve change factors and applying these factors to stations with an appropriate historical record included in the National Oceanic and Atmospheric Administration's Atlas 14 data product of point-based precipitation frequency estimates. To reflect the range of plausible changes for IDF curves in the future, the research team incorporated four downscaled climate model datasets, each generated from multiple global climate models, and two future scenarios. Because no single dataset or methodology can fully represent complex hydrological systems, whether historic or projected, a wide range of projected time series is critical to consider for planning and design. To make study results available to a broad regional audience, the research team produced (1) station-based projected IDF curves, based on county-level IDF curve change factors, for two future time periods for the CBW and Virginia and their uncertainty ranges and (2) an interactive online tool that allows end users to navigate these data. This report describes the project's motivation, data, and methodology and provides an overview of the results and interactive online tool. The aim of the report is to make the project's approach clear and transparent to those using the interactive online IDF curve tool and to those interested in replicating these methods in other contexts.

Contents

Preface	iii
Abstract.....	v
Figures	vii
Tables	viii
Acknowledgments	ix
Abbreviations	x
1. Introduction	1
Generating Climate Change–Informed IDF Curves	2
Study Objectives and Outcomes	5
Organization of This Report.....	6
2. Regional Context.....	7
Chesapeake Bay Watershed	7
Commonwealth of Virginia.....	9
3. Data.....	11
Station-Based Data.....	12
Downscaled Climate Model Datasets	13
Coupled Model Intercomparison Project 6	16
4. Methods	17
Step 1. Station-Based Atlas 14 IDF Curves.....	17
Step 2. Downscaled Climate Model Data IDF Curves	20
Partial Duration Series	20
L-moments	21
Step 3. Climate Change–Informed IDF Curve Change Factors.....	26
Step 4. Uncertainty Bounds for IDF Curve Change Factors.....	30
Step 5. County-Level Change Factors with Uncertainty Bounds	31
5. Results and Data Tool	33
Accessing IDF Curve Change Factors and Using the Data Tool.....	39
Recommended Application of Change Factors	40
6. Summary and Conclusions	41
References	44

Figures

Figure 2.1. Map of the Chesapeake Bay Watershed	8
Figure 4.1. Differences Between One-Day (converted to 24-hour) Atlas 14 and Project- Computed Recurrence Interval Rainfall Amounts	19
Figure 4.2. Quantile and Density Plots of the Fit GEV Distribution Using L-Moments, MLE, and GMLE.....	24
Figure 4.3. Ratio of Change Factors Calculated with Regional L-moments to Single-Grid L-Moments for NA-CORDEX (RCP 8.5, 2050–2099) (y axis), for Each Recurrence Interval (x axis).....	26
Figure 4.4. Analysis of Sub-Daily NA-CORDEX (50 km) Change Factors for RCP 8.5 (2050–2099)	29
Figure 4.5. Variance in Grid Cell Change Factors by County Across Study Region for the 100-Year Recurrence Interval	32
Figure 5.1. County-Level Change Factors for the CBW Projected by the Ensemble Median of All GCMs in Each Dataset for Both Future Periods Under RCP 4.5	35
Figure 5.2. County-Level Change Factors for the CBW Projected by the Ensemble Median of All GCMs in Each Dataset for Both Future Periods Under RCP 8.5	36
Figure 5.3. County-Level Change Factors for Virginia Projected by the Ensemble Median of All GCMs in Each Dataset for Both Future Periods Under RCP 4.5	37
Figure 5.4. County-Level Change Factors for Virginia Projected by the Ensemble Median of All GCMs in Each Dataset for Both Future Periods Under RCP 8.5	38
Figure 5.5. 2-Year Recurrence Interval IDF Curve for State College, Pennsylvania, Under RCP 4.5 from 2020 Through 2070	39

Tables

Table 3.1. Downscaled Climate Model Datasets Utilized in This Study	15
Table 4.1. Percentages of Study Area Where MLE or GMLE Performed Better, According to the AIC for LOCA.....	22
Table 4.2. Percentages of Study Area Where MLE or GMLE Performed Better, According to the AIC for NA-CORDEX (50 km)	23
Table 4.3. Average Ratio of Change Factors Calculated with Regional L-moments to Single-Grid L-Moments for NA-CORDEX (RCP 8.5, 2050–2099), for Each Recurrence Interval	25
Table 5.1. Study Area Averaged Ensemble Median Change Factors for Each Recurrence Interval, RCP, Future Period, and Downscaled Climate Model Dataset.....	33

Acknowledgments

The authors would like to acknowledge the funders of this work—the Chesapeake Bay Trust; the Virginia Transportation Research Council; and the Commonwealth Center for Recurrent Flooding Resiliency, managed by the Virginia Institute of Marine Science (VIMS), Old Dominion University (ODU) and the Virginia Coastal Policy Center—as well as the Mid-Atlantic Regional Integrated Sciences and Assessments program for supporting the publication of this report. This project was also made possible by the ongoing support and substantial contributions from our partner at the Chesapeake Bay Program—Urban Stormwater Workgroup Lead Normand Goulet (Northern Virginia Regional Commission)—as well as Senior Program Officer Sarah Koser and Director of Programs for Restoration Sadie Drescher from the Chesapeake Bay Trust. We would also like to thank Rear Admiral Ann Phillips, United States Navy (Retired), special assistant to the governor for coastal adaptation and protection for the Commonwealth of Virginia; Mark Luckenbach and Molly Mitchell from VIMS; Emily Steinhilber from ODU; and Chris Swanson and Alex Foraste from the Virginia Department of Transportation for their input and support for the Virginia components of this project. David Wood from the Chesapeake Stormwater Network and Katherine Filippino from the Hampton Roads Planning District Commission also made helpful contributions to tool development and outreach. We are also incredibly grateful to the two programmers from Cornell University—Adrien Zheng and Benjamin Eck—who led the web development for the online tool. Finally, we would like to thank the reviewers of this report—members of the Chesapeake Bay Program’s Urban Stormwater and Modeling Workgroups—for their significant contributions to clarifying and augmenting our project reporting and communication.

Abbreviations

AIC	Akaike Information Criterion
AMS	annual maximum series
BCCA _{v2}	Bias-Correction and Constructed Analogs version 2
CBW	Chesapeake Bay Watershed
CMIP5	Coupled Model Intercomparison Project 5
CMIP6	Coupled Model Intercomparison Project 6
CMU	Carnegie Mellon University
COOP	Cooperative Observer Program
CSN	Chesapeake Stormwater Network
GCM	global climate model
GEV	Generalized Extreme Value
GMLE	Generalized Maximum Likelihood Estimator
IDF	intensity-duration-frequency
km	kilometer
LOCA	Localized Constructed Analogs
MACA	Multivariate Adaptive Constructed Analogs
MARISA	Mid-Atlantic Regional Integrated Sciences and Assessments
MLE	Maximum Likelihood Estimator
NA-CORDEX	North American Coordinated Regional Downscaling Experiment
NCEI	National Centers for Environmental Information
NOAA	National Oceanic and Atmospheric Administration
NRCC	Northeast Regional Climate Center
NWS	National Weather Service
ODU	Old Dominion University
PDS	partial duration series

PFDS	Precipitation Frequency Data Server
QDM	quantile delta method
RCC	Regional Climate Center
RCP	representative concentration pathway
USWG	Urban Stormwater Workgroup
VIMS	Virginia Institute of Marine Science

1. Introduction

During the summer of 2019, the Chesapeake Bay Watershed (CBW) and parts of Virginia experienced historic flash flooding and extreme precipitation events, including the issuance of two rare National Weather Service (NWS) flash flood emergencies. On June 29–30, 2019, for example, western Maryland and eastern West Virginia saw up to five inches of rain, ranking as the region’s second-wettest day since 1902 at one site in the region. On July 8, 2019, a rain gauge at Ronald Reagan National Airport near Washington, D.C., recorded 3.30 inches of rain in one hour, hitting another record for the largest one-hour rainfall total over the past 60 years. The severity of the July 8 event in the D.C. metropolitan area led to significant localized flooding of roadways and rapid rises in waterways, with Four Mile Run in Arlington, Virginia, for example, rising more than 11 feet in one hour. The summer of 2019 also brought a 500-year storm event to Baltimore, Maryland, and another storm that dropped 2 inches of rain on Norfolk, Virginia, within 31 minutes.² Both resulted in significant flooding. The 2019 season was not an isolated occurrence in the historic record. It instead exemplifies an ongoing trend of increasing rainfall extremes and resulting urban and riverine flood damage across the region.³

Similar to the events of summer 2019, over the past decade, the CBW and Virginia have experienced increases in the frequency and intensity of extreme precipitation compared with historical averages, as well as changes in seasonal total precipitation.^{4 5} Moreover, research examining downscaled global climate model (GCM) output has also shown that these trends are anticipated to continue to grow over the next several decades by the middle to late 21st century.⁶ As a result, urban and coastal flooding could be magnified and more frequent in the future in the absence of adaptation. This presents stormwater engineers and planners with a key challenge—how to incorporate these recent and future changes in precipitation into stormwater infrastructure design and management.

² Michelle E. Miro, Krista Romita Grocholski, Samantha Borisoff, Jordan R. Fischbach, and Arthur T. DeGaetano, “Chesapeake Bay Watershed Climate Impacts Summary and Outlook: Summer 2019,” Mid-Atlantic Regional Integrated Sciences and Assessments, 2019.

³ Jordan R. Fischbach, Michelle E. Miro, Lauren Kendrick, and Arthur T. DeGaetano, “Chesapeake Bay Watershed Climate Impacts Summary and Outlook for 2018,” Mid-Atlantic Regional Integrated Sciences and Assessment, 2018.

⁴ Jordan R. Fischbach, Michelle E. Miro, Lauren Kendrick, and Arthur T. DeGaetano, “Chesapeake Bay Watershed Climate Impacts Summary and Outlook for 2018,” Mid-Atlantic Regional Integrated Sciences and Assessment, 2018.

⁵ Jordan R. Fischbach, Michelle E. Miro, Krista Romita Grocholski, Arthur T. DeGaetano, and Samantha Borisoff, “Chesapeake Bay Watershed Climate Impacts Summary and Outlook: Winter 2018–2019,” Mid-Atlantic Regional Integrated Sciences and Assessment, 2019.

⁶ Jordan R. Fischbach, Michelle E. Miro, Lauren Kendrick, and Arthur T. DeGaetano, “Chesapeake Bay Watershed Climate Impacts Summary and Outlook for 2018,” Mid-Atlantic Regional Integrated Sciences and Assessment, 2018.

Stormwater engineering design and management relies heavily on hydrologic methods and measures that utilize historic precipitation records. Intensity-duration-frequency (IDF) curves are one such foundational method that are used across a broad set of water resource engineering applications, ranging from small to large infrastructure (e.g., from culverts to dams). IDF curves represent the relationship between (1) intensity (inches per hour) or depth (inches); (2) the duration of a rainfall event (anywhere from a few minutes to a few days but typically 1–24 hours); and (3) an empirical measure of frequency, representing the average time between occurrences (such as once in a hundred years, or a 1-percent chance each year). IDF curves are derived from historic rainfall data, typically observed rainfall data from rain gauges; there is no single method for developing IDF curves from historic rainfall data. Within common hydrologic practice, there are a range of approaches and decision points along the IDF curve derivation process, such as the treatment of the precipitation time series (e.g., partial duration series [PDS]) or the selection of the method to fit the extreme value distribution (e.g., L-moments).⁷

The National Oceanic and Atmospheric Administration (NOAA) has standardized one approach to deriving IDF curves with the publication of NOAA Atlas 14: Precipitation-Frequency Atlas of the United States (Atlas 14).⁸ Although some localities still choose to derive their own IDF curves, Atlas 14 is the dominant source for IDF curves for jurisdictions across the United States. Atlas 14 is based on historic station-based observations of rainfall and relies on all years available in the record. Atlas 14 was produced in 2006 for the majority of the CBW, and Virginia and does not incorporate rainfall data observed after 2000 into its IDF curves. The Atlas 14 methodology also relies on assumptions of stationarity—that the variability seen in the historic record does not vary with time.⁹ However, many regions within the CBW and Virginia have seen increases in extreme precipitation in recent years, and changes are expected to continue to grow into the future. These two key limitations of Atlas 14—the time period used for analysis and assumptions of stationarity—could thus lead to underestimation of precipitation extremes when designing infrastructure for the future.

Generating Climate Change–Informed IDF Curves

To overcome the limitations of traditional methods for generating IDF curves, similar to those highlighted above for Atlas 14, researchers and practitioners have developed several different approaches to account for nonstationarity and plausible future changes in rainfall in IDF

⁷ V. Te Chow, D. R. Maidment, and L. W. Mays, “Applied Hydrology,” *Journal of Engineering Education*, Vol. 308, 1962, p. 1959.

⁸ Geoffrey M. Bonnin, Deborah Martin, Bingzhang Lin, Tye Parzybok, Michael Yekta, and David Riley, *NOAA Atlas 14: Precipitation-Frequency Atlas of the United States, Vol. 2, Version 3.0: Delaware, District of Columbia, Illinois, Indiana, Kentucky, Maryland, New Jersey, North Carolina, Ohio, Pennsylvania, South Carolina, Tennessee, Virginia, West Virginia*, Silver Spring, Md.: U.S. Department of Commerce, National Oceanic and Atmospheric Administration, and National Weather Service, 2006.

⁹ P. C. D. Milly, Julio Betancourt, Malin Falkenmark, Robert M. Hirsch, Zbigniew W. Kundzewicz, Dennis P. Lettenmaier, and Ronald J. Stouffer, “Stationarity Is Dead: Whither Water Management?” *Science*, Vol. 319, No. 5863, February 1, 2008, pp. 573–574.

curve values. Among these approaches, there are generally two main areas of focus. The first of these adjusts the statistical methodology by allowing key parameters of the probability distribution to vary with variables known to have a relationship with rainfall, such as time, rather than being held constant.^{10 11 12} For example, in Agilan and Umamahesh, 2017,¹³ and Cheng and AghaKouchak, 2014,¹⁴ the authors introduce a mathematical relationship between the location parameter of the Generalized Extreme Value (GEV) distribution function and time, meaning that the distribution itself is dependent on time. In doing so, they address the assumption of stationarity—that variability in the rainfall record does not change with time. This group of methods does not generally incorporate future projections of precipitation but instead focuses on better characterizing the time-dependent variability in rainfall observed in the historic record.

The second group of methods incorporates estimates of future precipitation from GCMs as a part of the time series used to generate IDF curve values.^{15 16 17 18 19 20} Within this group, researchers from the University of Maryland derived IDF curves for cities within Maryland’s Eastern Shore directly from a frequency analysis of 30 years of precipitation outputs from the North American Regional Climate Change Assessment Project, a dynamically downscaled

¹⁰ V. Agilan and N. V. Umamahesh, “What Are the Best Covariates for Developing Non-Stationary Rainfall Intensity-Duration-Frequency Relationship?” *Advances in Water Resources*, Vol. 101, March 2017, pp. 11–22.

¹¹ Linyin Cheng and Amir AghaKouchak, “Nonstationary Precipitation Intensity-Duration-Frequency Curves for Infrastructure Design in a Changing Climate,” *Scientific Reports*, Vol. 4, November 2014.

¹² Ali Sarhadi and Eric D. Soulis, “Time-Varying Extreme Rainfall Intensity-Duration-Frequency Curves in a Changing Climate,” *Geophysical Research Letters*, Vol. 44, No. 5, March 16, 2017, pp. 2454–2463.

¹³ V. Agilan and N. V. Umamahesh, “What Are the Best Covariates for Developing Non-Stationary Rainfall Intensity-Duration-Frequency Relationship?” *Advances in Water Resources*, Vol. 101, March 2017, pp. 11–22.

¹⁴ Linyin Cheng and Amir AghaKouchak, “Nonstationary Precipitation Intensity-Duration-Frequency Curves for Infrastructure Design in a Changing Climate,” *Scientific Reports*, Vol. 4, November 2014.

¹⁵ Lauren M. Cook, Christopher J. Anderson, and Constantine Samaras, “Framework for Incorporating Downscaled Climate Output into Existing Engineering Methods: Application to Precipitation Frequency Curves,” *Journal of Infrastructure Systems*, Vol. 23, No. 4, December 2017.

¹⁶ Arthur T. DeGaetano and Christopher M. Castellano, “Future Projections of Extreme Precipitation Intensity-Duration-Frequency Curves for Climate Adaptation Planning in New York State,” *Climate Services*, Vol. 5, January 2017, pp. 23–35.

¹⁷ Elisa Ragno, Amir AghaKouchak, Charlotte A. Love, Linyin Cheng, Farshid Vahedifard, and Carlos H. R. Lima, “Quantifying Changes in Future Intensity-Duration-Frequency Curves Using Multimodel Ensemble Simulations,” *Water Resources Research*, Vol. 54, No. 3, 2018, pp. 1751–1764.

¹⁸ Shu Wu, Momcilo Markus, David Lorenz, James R. Angel, and Kevin Grady, “A Comparative Analysis of the Historical Accuracy of the Point Precipitation Frequency Estimates of Four Data Sets and Their Projections for the Northeastern United States,” *Water*, Vol. 11, No. 6, 2019, p. 1279.

¹⁹ Jonathan B. Butcher, Tan Zi, Brian R. Pickard, Scott C. Job, Thomas E. Johnson, and Bryan A. Groza, “Efficient Statistical Approach to Develop Intensity-Duration-Frequency Curves for Precipitation and Runoff Under Future Climate,” *Climatic Change*, Vol. 164, No. 1, 2021, pp. 1–20.

²⁰ Michelle Charochak and James Bass, *Preparing for Increases in Extreme Precipitation Events in Local Planning and Policy on Maryland’s Eastern Shore*, a report prepared for the Eastern Shore Climate Adaptation Partnership by Eastern Shore Land Conservancy, January 2020.

gridded climate model dataset available at a 50-kilometer (km) resolution.²¹ Ragno et al., 2018, relied on downscaled climate model data from Bias-Correction and Constructed Analogs version 2 (BCCAv2) to generate modeled historic and projected future IDF curves. Historic IDF curves were compared with Atlas 14 values at the relevant sites, and any bias between historic modeled and Atlas 14 values was removed from the future IDF curves.²² DeGaetano and Castellano, 2017, developed future IDF curves for New York State using a range of downscaled climate model datasets to derive modeled historic and future IDF curves, compute change factors between historic and future values, and apply these change factors to IDF curves based on observed rainfall data.²³ Butcher et al., 2021, took a hybrid approach that adjusts the extreme value fit used to generate IDF curve values with equidistant quantile mapping, which compares both the location and scale of the change in downscaled climate model estimates of rainfall between historic and future conditions.²⁴

The existing and ongoing work around developing nonstationary and projected IDF curves shows that no single, standardized method exists and that those researchers utilizing climate model data have worked with a range of GCMs and downscaled climate model datasets. Yet, the data and methodological choices matter. Research has shown that the choice of downscaled climate model dataset and the various modeling choices made to derive IDF curve values lead to important differences in the resulting IDF curves.²⁵ ²⁶ At the same time, rather than working to pick the “right” single future climate projection, GCM, or methodology, it is important to characterize the uncertainty in future IDF curves, or the plausible range of IDF curve values taking into account the variability in values derived from different methods or input datasets.

Although much of the IDF curve literature focuses on uncertainty introduced through statistical methods to resample either the input historical data time series or the extreme value distribution (e.g., bootstrapping), future projected IDF curves introduce additional uncertainties. These additional uncertainties are predominantly due to the choice of GCMs, the future emissions scenario that drives GCM output, and the downscaling method applied to rescale

²¹ Michelle Charochak and James Bass, *Preparing for Increases in Extreme Precipitation Events in Local Planning and Policy on Maryland’s Eastern Shore*, a report prepared for the Eastern Shore Climate Adaptation Partnership by Eastern Shore Land Conservancy, January 2020.

²² Elisa Ragno, Amir AghaKouchak, Charlotte A. Love, Linyin Cheng, Farshid Vahedifard, and Carlos H. R. Lima, “Quantifying Changes in Future Intensity-Duration-Frequency Curves Using Multimodel Ensemble Simulations,” *Water Resources Research*, Vol. 54, No. 3, 2018, pp. 1751–1764.

²³ Arthur T. DeGaetano and Christopher M. Castellano, “Future Projections of Extreme Precipitation Intensity-Duration-Frequency Curves for Climate Adaptation Planning in New York State,” *Climate Services*, Vol. 5, January 2017, pp. 23–35.

²⁴ Jonathan B. Butcher, Tan Zi, Brian R. Pickard, Scott C. Job, Thomas E. Johnson, and Bryan A. Groza, “Efficient Statistical Approach to Develop Intensity-Duration-Frequency Curves for Precipitation and Runoff Under Future Climate,” *Climatic Change*, Vol. 164, No. 1, 2021, pp. 1–20.

²⁵ Lauren M. Cook, Seth McGinnis, and Constantine Samaras, “The Effect of Modeling Choices on Updating Intensity-Duration-Frequency Curves and Stormwater Infrastructure Designs for Climate Change,” *Climatic Change*, Vol. 159, No. 2, 2020, pp. 289–308.

²⁶ Tania López-Cantú, Andreas F. Prein, and Constantine Samaras, “Uncertainties in Future U.S. Extreme Precipitation from Downscaled Climate Projections,” *Geophysical Research Letters*, Vol. 47, No. 9, May 16, 2020.

GCM output to a higher spatial resolution more relevant for localized precipitation analyses. Because both data and methodological choices can contribute to uncertainty, a range of methods and data are most usefully employed to characterize and communicate to planners and engineers the full spectrum of extreme precipitation conditions in the future.

Study Objectives and Outcomes

The objective of this study is to leverage the best available science to develop climate change–informed IDF curves that can be easily applied across the CBW and Virginia to plan, design, and build infrastructure assets consistent with anticipated future precipitation conditions. This approach stands in marked contrast to the common practice of basing infrastructure decisions on analyses with historical precipitation records alone. Although there are multiple means of carrying out this objective, the study team grounded this work in the following principles that have driven and informed method and data choice:

- Projected IDF curves should be relevant to the engineering community in a manner consistent with their current use—namely, they should be applicable to Atlas 14.
- Uncertainty ranges resulting from method and data choice should be clear and well characterized. No single dataset or methodology can fully represent a complex hydrological system, whether historic or projected.
- Methods should be transparent and reproducible.

To these ends and to support the use of future projected IDF curves, this study also produced the following items:

- projected IDF curves, based on IDF curve change factors (described in detail in Chapter 4) for two future time periods (2020–2069 and 2050–2099). IDF curve values and change factors are computed at 2-, 5-, 10-, 25-, 50-, and 100-year annual recurrence intervals for 5-minute to 7-day durations for the entire CBW and Virginia.
- an interactive online tool produced by developers at the Northeast Regional Climate Center (NRCC) that allows end users to navigate the final research products. This interactive tool makes available station-specific IDF curves and station-specific and county-level IDF curve change factors, as well as this technical project report. This tool can be accessed at <https://midatlantic-idf.rcc-acis.org>.²⁷
- a recorded webinar that provides an overview of the study and its methods and walks viewers through how to use the online tool. This webinar is available for online viewing via the webpage hosting the interactive online tool.
- several draft academic journal articles that highlight the scientific contributions of this effort and put this work in the context of a larger body of scientific research through a detailed and comprehensive literature review. As these articles are

²⁷ Mid-Atlantic Regional Integrated Sciences and Assessments, “Projected Intensity-Duration-Frequency (IDF) Curve Data Tool for the Chesapeake Bay Watershed and Virginia,” undated.

submitted and published (publication dates are anticipated after completion of this report), they will be cited and linked in the online tool.

Organization of This Report

This report details the project's data, approach, and results and is intended to make the project's methodology clear and transparent to those using the IDF curve tool and those interested in replicating these methods in other contexts. Chapter 2 describes the regional context of the CBW and Virginia. Chapter 3 describes data used to produce the study results and provides pertinent details on the relevance of this work. In Chapter 4, the methodology employed to derive future projected IDF curves and their uncertainty bounds is explained. Chapter 5 provides an overview of the results of this methodology and how to use and access the full study results from the interactive tool. Chapter 6 offers final reflections on methods, results, and next steps.

The scope of this study was centered around the production of future projected IDF curves and ensuring that they were accessible online and based on transparent methods. As such, we did not include a deep academic-style literature review in this report and focused instead on the technical details of the data choice and methodology, noting relevant peer-reviewed literature that underpins the methods. A detailed and comprehensive literature review and thorough analysis of the results are included in draft scientific articles prepared for submission.

2. Regional Context

Chesapeake Bay Watershed

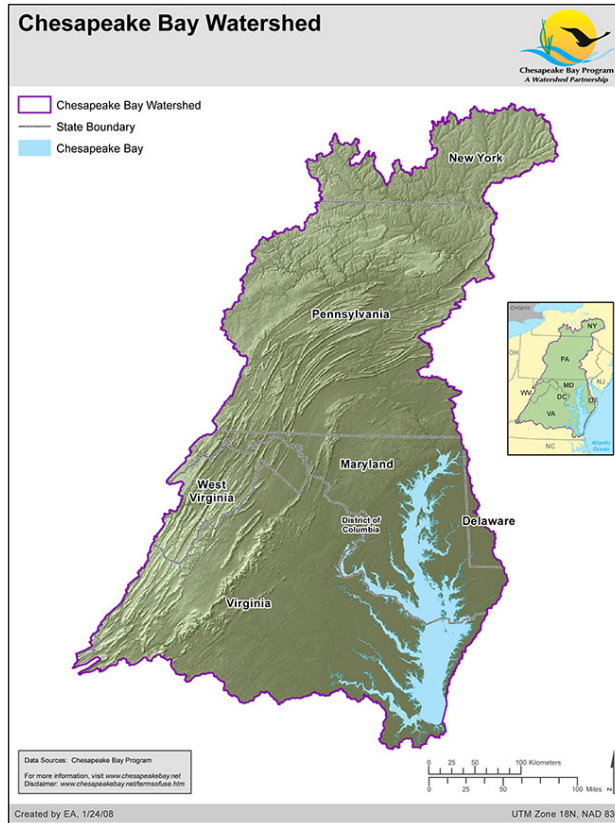
The Chesapeake Bay Watershed (CBW) is the largest estuary in the United States. It spans 64,000 square miles, covering portions of six states and the District of Columbia (Figure 2.1). More than 18 million people live within its boundaries.²⁸ Between its significant water resources and large population centers, stormwater issues have long been a concern for the CBW. Exacerbating these stormwater issues, the CBW has experienced increases in extreme precipitation events over the past decade compared with historical averages, with the greatest increases seen in the most extreme events (i.e., days with a total of at least 2 inches of rainfall).²⁹ Projections of future climate show that these extreme precipitation events will increase further in the coming decades. By the mid-21st century, the CBW “could experience a doubling of annual extreme precipitation events over 2 and 3 inches compared to historical averages.”³⁰ This suggests that urban flood events, similar to those described in the beginning of Chapter 1, will likely become more common in the future, placing considerable strain on existing stormwater infrastructure.

²⁸ Chesapeake Bay Foundation, “Geography and Facts,” webpage, undated.

²⁹ Jordan R. Fischbach, Michelle E. Miro, Lauren Kendrick, and Arthur T. DeGaetano, “Chesapeake Bay Watershed Climate Impacts Summary and Outlook for 2018,” Mid-Atlantic Regional Integrated Sciences and Assessment, 2018.

³⁰ Jordan R. Fischbach, Michelle E. Miro, Lauren Kendrick, and Arthur T. DeGaetano, “Chesapeake Bay Watershed Climate Impacts Summary and Outlook for 2018,” Mid-Atlantic Regional Integrated Sciences and Assessment, 2018.

Figure 2.1. Map of the Chesapeake Bay Watershed



SOURCE: Chesapeake Bay Foundation, "The Chesapeake Bay Watershed," January 24, 2008.

Several groups have been working to address these concerns. In particular, the Chesapeake Bay Program’s Urban Stormwater Workgroup (USWG) was established in 2000 to engage with local governments to “encourage the development and implementation of emerging urban stormwater practices.”³¹ In support of the USWG, the Chesapeake Stormwater Network (CSN) recently completed a series of four reports for the Chesapeake Bay Program that are focused on stormwater issues in the watershed. These reports illuminate a number of key points relevant for this study. First, they found that there is no consistent regional approach to stormwater management, with no two states using the same engineering design standards.³² Second, in addition to each state using disparate approaches to stormwater design and management, entities within states (departments of transportation, environmental regulatory agencies, etc.) do not use and discuss precipitation data and design storms in a consistent manner.³³ Finally, CSN reported

³¹ Chesapeake Bay Program, “Urban Stormwater Workgroup,” webpage, undated.

³² A summary of each state’s design standards can be found in Appendix A of the following report: David Wood, *Review of Current Stormwater Engineering Standards and Criteria for Rainfall and Runoff Modeling in the Chesapeake Bay Watershed*, Chesapeake Stormwater Network, 2020.

³³ David Wood, *Review of Current Stormwater Engineering Standards and Criteria for Rainfall and Runoff Modeling in the Chesapeake Bay Watershed*, Chesapeake Stormwater Network, 2020.

on the results of a survey that found that, because of recent and ongoing climate changes, “less than 10% of respondents [were] comfortable with the current engineering design criteria” that they had access to, and they were generally open to using new tools, particularly updated or projected IDF curves.³⁴

In addition to the need for updated design standards that reflect recent and ongoing climate change, the region’s lack of a consistent approach introduces additional complications and uncertainty into stormwater planning and management. Given willingness across the region to use new stormwater management tools, the consistent set of projected IDF curves produced by this study can serve as a resource to mitigate the impact of some of the region’s stormwater management challenges.

Commonwealth of Virginia

The Commonwealth of Virginia, overall, has experienced similar extreme precipitation events and resulting stormwater issues that affect the rest of the CBW. Based on data from the Third National Climate Assessment, Runkle et al., 2017, found an upward trend in the number of extreme precipitation events in recent decades (1995–2014 in their study). Interestingly, they also found no trend in the total annual precipitation over that same period.³⁵ This could indicate that, in the recent past, more of Virginia’s precipitation has come in the form of extreme events. By the mid-21st century, climate projections suggest that the number of days with extreme precipitation (i.e., days with a total of at least 2 inches of rain) will increase by 50–100 percent for much of the state.³⁶

Individual localities have conducted studies with detailed hydraulic and hydrologic models to better understand how these extreme events might impact their communities. One example of such a study was completed by Dewberry for the City of Virginia Beach. That study’s final recommendation was, over a 40-year planning horizon, to increase existing design guidelines by 20 percent based on results of an analysis of future climate projections.³⁷ That study directly informed climate resilient stormwater management for Virginia Beach, Virginia. It is likely not feasible for all communities within Virginia to conduct such a detailed analysis on their own.³⁸

³⁴ David Wood and Tom Schueler, *Summary of Stakeholder Concerns, Current Management and Future Needs for Addressing Climate Change Impacts on Stormwater Management*, Chesapeake Stormwater Network, 2020.

³⁵ Jennifer Runkle, Kenneth E. Kunkel, Laura Stevens, Sarah Champion, Brooke C. Stewart, Rebekah Frankson, and William Sweet, *2017: Virginia State Climate Summary*, NOAA Technical Report NESDIS 149-VA, 2017.

³⁶ Jordan R. Fischbach, Michelle E. Miro, Lauren Kendrick, and Arthur T. DeGaetano, “Chesapeake Bay Watershed Climate Impacts Summary and Outlook for 2018,” Mid-Atlantic Regional Integrated Sciences and Assessment, 2018.

³⁷ Dmitry Smirnov, Jason Giovannettone, Seth Lawler, Mathini Sreetharan, Joel Plummer, Brad Workman, and Brian Batten, *Analysis of Historical and Future Heavy Precipitation, City of Virginia Beach, Virginia*, Virginia Beach, Va.: Department of Public Works, 2018.

³⁸ Jim Parsons, “Virginia Beach Makes Plans to Keep Its Head Above Water,” *Engineering News Record*, April 28, 2019.

This report constitutes a consistent resource to enable communities across Virginia to explore anticipated changes across design storms, as well as access future change factors that can be applied to existing design guidelines.

3. Data

The core data in this study are historic and projected precipitation data used to generate IDF curves and their future change factors (this methodology is explained in detail in Chapter 4). These datasets include both station-based observations of past precipitation and modeled historic and projected precipitation from downscaled climate model datasets. For station data, we drew from the network of stations that is available in Atlas 14,³⁹ ⁴⁰ but we used data only from the stations with an appropriate historic record. For modeled precipitation data, we utilized downscaled climate model datasets that are widely used in climate change studies on precipitation and prior work on developing future projected IDF curves.⁴¹ ⁴² ⁴³

Specifically, these datasets included

- station-based precipitation data from the NWS Cooperative Observer Program (COOP) Network⁴⁴
- modeled precipitation data from the North American Coordinated Regional Downscaling Experiment (NA-CORDEX),⁴⁵ Multivariate Adaptive Constructed Analogs (MACA),⁴⁶ Localized Constructed Analogs (LOCA),⁴⁷ and BCCAv2.⁴⁸

³⁹ Geoffrey M. Bonnin, Deborah Martin, Bingzhang Lin, Tye Parzybok, Michael Yekta, and David Riley, *NOAA Atlas 14: Precipitation-Frequency Atlas of the United States, Vol. 2, Version 3.0: Delaware, District of Columbia, Illinois, Indiana, Kentucky, Maryland, New Jersey, North Carolina, Ohio, Pennsylvania, South Carolina, Tennessee, Virginia, West Virginia*, Silver Spring, Md.: U.S. Department of Commerce, National Oceanic and Atmospheric Administration, and National Weather Service, 2006.

⁴⁰ Sanja Perica, Sandra Pavlovic, Michael St. Laurent, Carl Trypaluk, Dale Unruh, Deborah Martin, and Orlan Wilhite, *NOAA Atlas 14: Precipitation-Frequency Atlas of the United States, Vol. 10, Version 3.0, Northern States: Connecticut, Maine, Massachusetts, New Hampshire, New York, Rhode Island, Vermont*, Silver Spring, Md.: U.S. Department of Commerce, National Oceanic and Atmospheric Administration, and National Weather Service, 2019.

⁴¹ Shu Wu, Momcilo Markus, David Lorenz, James R. Angel, and Kevin Grady, “A Comparative Analysis of the Historical Accuracy of the Point Precipitation Frequency Estimates of Four Data Sets and Their Projections for the Northeastern United States,” *Water*, Vol. 11, No. 6, 2019, p. 1279.

⁴² Tania López-Cantú, Andreas F. Prein, and Constantine Samaras, “Uncertainties in Future U.S. Extreme Precipitation from Downscaled Climate Projections,” *Geophysical Research Letters*, Vol. 47, No. 9, May 16, 2020.

⁴³ Arthur T. DeGaetano and Christopher M. Castellano, “Future Projections of Extreme Precipitation Intensity-Duration-Frequency Curves for Climate Adaptation Planning in New York State,” *Climate Services*, Vol. 5, January 2017, pp. 23–35.

⁴⁴ National Weather Service, “Cooperative Observer Program (COOP),” webpage, undated.

⁴⁵ L. O. Mearns et al., *The NA-CORDEX Dataset*, Version 1.0, Boulder Colo.: NCAR Climate Data Gateway, 2017.

⁴⁶ John T. Abatzoglou and Timothy J. Brown, “A Comparison of Statistical Downscaling Methods Suited for Wildfire Applications,” *International Journal of Climatology*, Vol. 32, Vol. 5, April 2012, pp. 772–780.

⁴⁷ David W. Pierce, Daniel R. Cayan, and Bridget L. Thrasher, “Statistical Downscaling Using Localized Constructed Analogs (LOCA),” *Journal of Hydrometeorology*, Vol. 15, No. 6, 2014, pp. 2558–2585.

⁴⁸ D. Maraun, F. Wetterhall, A. M. Ireson, R. E. Chandler, E. J. Kendon, M. Widmann, S. Brienen, H. W. Rust, T. Sauter, M. Themeßl, V. K. C. Venema, K. P. Chun, C. M. Goodess, R. G. Jones, C. Onof, M. Vrac, and I. Thiele-

Station-Based Data

Daily precipitation data from stations across the CBW and Virginia were obtained from the NWS COOP network stations available from the Applied Climate Information System. This is the same base dataset that the NRCC used to produce updated IDF curves for the Natural Resources Conservation Service and the State of New York,⁴⁹ and it overlaps with stations used to generate IDF curves in Atlas 14.^{50 51} The procedure for extracting and refining these data to the needs of this study included the following steps: Daily COOP network stations within the area extending from 46.0°N to 36.0°N and 84.0°W to 71.0°W were identified. From these locations, a set of 480 base sites was retained based on the following criteria: (1) The site was included in NOAA Atlas 14 Volume 2⁵² or Volume 10;⁵³ (2) the site contains a data record that extends from at least 1950 through 2019; and (3) the site has less than 5 percent of daily precipitation data missing. Similarly, a larger set of regional stations was retained that included the base stations and additional sites with at least 20 years of record after 1980. For all sites, daily rainfall observations and any associated data flags were extracted and reflect the values in the Global Historical Climatology Network. The data used reflect those available on January 13, 2021. More detail on these data can be found at https://www.rcc-acis.org/docs_datasets.html.⁵⁴

Similar criteria were used to select 85 hourly observing stations. These sites were extracted from one of three databases: (1) NOAA National Centers for Environmental Information (NCEI)

Eich, “Precipitation Downscaling Under Climate Change: Recent Developments to Bridge the Gap Between Dynamical Models and the End User,” *Reviews of Geophysics*, Vol. 48, No. 3, September 2010.

⁴⁹ Arthur T. DeGaetano and Christopher M. Castellano, “Future Projections of Extreme Precipitation Intensity-Duration-Frequency Curves for Climate Adaptation Planning in New York State,” *Climate Services*, Vol. 5, January 2017, pp. 23–35.

⁵⁰ Geoffrey M. Bonnin, Deborah Martin, Bingzhang Lin, Tye Parzybok, Michael Yekta, and David Riley, *NOAA Atlas 14: Precipitation-Frequency Atlas of the United States, Vol. 2, Version 3.0: Delaware, District of Columbia, Illinois, Indiana, Kentucky, Maryland, New Jersey, North Carolina, Ohio, Pennsylvania, South Carolina, Tennessee, Virginia, West Virginia*, Silver Spring, Md.: U.S. Department of Commerce, National Oceanic and Atmospheric Administration, and National Weather Service, 2006.

⁵¹ Sanja Perica, Sandra Pavlovic, Michael St. Laurent, Carl Trypaluk, Dale Unruh, Deborah Martin, and Orlan Wilhite, *NOAA Atlas 14: Precipitation-Frequency Atlas of the United States, Vol. 10, Version 3.0, Northern States: Connecticut, Maine, Massachusetts, New Hampshire, New York, Rhode Island, Vermont*, Silver Spring, Md.: U.S. Department of Commerce, National Oceanic and Atmospheric Administration, and National Weather Service, 2019.

⁵² Geoffrey M. Bonnin, Deborah Martin, Bingzhang Lin, Tye Parzybok, Michael Yekta, and David Riley, *NOAA Atlas 14: Precipitation-Frequency Atlas of the United States, Vol. 2, Version 3.0: Delaware, District of Columbia, Illinois, Indiana, Kentucky, Maryland, New Jersey, North Carolina, Ohio, Pennsylvania, South Carolina, Tennessee, Virginia, West Virginia*, Silver Spring, Md.: U.S. Department of Commerce, National Oceanic and Atmospheric Administration, and National Weather Service, 2006.

⁵³ Sanja Perica, Sandra Pavlovic, Michael St. Laurent, Carl Trypaluk, Dale Unruh, Deborah Martin, and Orlan Wilhite, *NOAA Atlas 14: Precipitation-Frequency Atlas of the United States, Vol. 10, Version 3.0, Northern States: Connecticut, Maine, Massachusetts, New Hampshire, New York, Rhode Island, Vermont*, Silver Spring, Md.: U.S. Department of Commerce, National Oceanic and Atmospheric Administration, and National Weather Service, 2019.

⁵⁴ Applied Climate Information System, “Datasets,” webpage, 2017.

COOP-Hourly Precipitation Data Version 2 for stations with available records after 2014;⁵⁵ (2) NCEI’s Hourly Precipitation Dataset, known historically as DSI-3240,⁵⁶ for stations with records ending prior to 2014; and (3) NCEI Surface Data Hourly Global (DS3505)⁵⁷ for NWS Automated Surface Observing System stations.

Downscaled Climate Model Datasets

GCM projections and historical simulations are a widely used source of information about our changing climate. GCM output data are available from a suite of 35 global scale models run under consistent scenarios of future atmospheric greenhouse gas concentrations, termed representative concentration pathways (RCPs), and made available by the World Climate Research Programme on the Program for Climate Model Diagnosis and Intercomparison website.^{58 59} This suite of models and RCPs are referred to as the Coupled Model Intercomparison Project Phase 5 (CMIP5) simulations. CMIP5 historical simulations of daily precipitation are available from 1950 through 2005, and CMIP5 projections of future precipitation are available from 2006 through 2100 for most GCMs.⁶⁰

Future projections are computed under four RCPs—RCP 2.6, RCP 4.5, RCP 6.0, and RCP 8.5—named by the radiative forcing values that these scenarios are developed to simulate.⁶¹ More information on CMIP5 models and RCPs can be found in Taylor et al., 2012.⁶² This report uses two of these four RCPs: RCP 4.5 and RCP 8.5. RCP 4.5 was designed to represent an intermediate scenario of future atmospheric concentrations of greenhouse gas emissions, characterized by a stabilizing of emissions over time.⁶³ RCP 8.5 represents high levels of

⁵⁵ David Wuertz, Jay Lawrimore, and Bryant Korzeniewski, *Cooperative Observer Program (COOP) Hourly Precipitation Data (HPD)*, Version 2.0, NOAA National Centers for Environmental Information, 2018.

⁵⁶ NOAA National Centers for Environmental Information, “Hourly Precipitation Data,” webpage, undated.

⁵⁷ Data.gov, “Integrated Surface Global Hourly Data,” National Climatic Data Center, 2021.

⁵⁸ Karl E. Taylor, Ronald J. Stouffer, and Gerald A. Meehl, “An Overview of CMIP5 and the Experiment Design,” *Bulletin of the American Meteorological Society*, Vol. 93, No. 4, 2012, pp. 485–498.

⁵⁹ Lawrence Livermore National Laboratory, “Program for Climate Model Diagnosis and Intercomparison,” webpage, 2021.

⁶⁰ Karl E. Taylor, Ronald J. Stouffer, and Gerald A. Meehl, “An Overview of CMIP5 and the Experiment Design,” *Bulletin of the American Meteorological Society*, Vol. 93, No. 4, 2012, pp. 485–498.

⁶¹ Detlef P. van Vuuren, Jae Edmonds, Mikiko Kainuma, Keywan Riahi, Allison Thomson, Kathy Hibbard, George C. Hurtt, Tom Kram, Volker Krey, Jean-Francois Lamarque, Toshihiko Masui, Malte Meinshausen, Nebojsa Nakicenovic, Steven J. Smith, and Steven K. Rose, “The Representative Concentration Pathways: An Overview,” *Climatic Change*, Vol. 109, No. 5, 2011.

⁶² Karl E. Taylor, Ronald J. Stouffer, and Gerald A. Meehl, “An Overview of CMIP5 and the Experiment Design,” *Bulletin of the American Meteorological Society*, Vol. 93, No. 4, 2012, pp. 485–498.

⁶³ Allison M. Thomson, Katherine V. Calvin, Steven J. Smith, G. Page Kyle, April Volke, Pralit Patel, Sabrina Delgado-Arias, Ben Bond-Lamberty, Marshall A. Wise, Leon E. Clarke, and James A. Edmonds, “RCP4.5: A Pathway for Stabilization of Radiative Forcing by 2100,” *Climatic Change*, Vol. 109, No. 77, 2011.

atmospheric greenhouse gases caused by increasing emissions to 2100.⁶⁴ These are the two most-used RCPs in climate adaptation literature and practice, often interpreted as an optimistic future with low emissions—RCP 4.5—and closer to a “worst case” future with higher emissions—RCP 8.5.

The output from the CMIP5 simulations is at a coarse global resolution, which limits the direct applicability to regional- or local-scale analyses, and additional methods are needed to relate coarse-scale GCM output to local scales. The process of rescaling GCMs is termed *downscaling* and generally consists of two main approaches: (1) statistical methods that derive empirical relationships between coarse-scale and finer resolution data and (2) dynamical methods that use models based on physical processes to generate finer-resolution data.⁶⁵ Both statistically and dynamically downscaled GCM datasets are widely used in the water resources and climate adaptation communities.

For this study, the research team selected four datasets that have been utilized and cited in prior projected IDF curve studies and cover an array of features that allowed us to explore the plausible range of future climate changes and uncertainty in method and model selection. These include NA-CORDEX,⁶⁶ BCCAv2,⁶⁷ LOCA,⁶⁸ and MACA.⁶⁹ Table 3.1 highlights the unique features of each of these datasets. For example, LOCA includes 32 of the 35 GCMs in the CMIP5 simulations for RCPs 4.5 and 8.5, while NA-CORDEX, the only dynamically downscaled dataset selected for this study, contains six GCMs from CMIP5. Because the downscaling approach, the GCM selection, the RCP, and the spatial and temporal resolutions each introduce their own source of uncertainty, it is important to consider a range of these features for this study to capture the plausible range in future IDF curves.

⁶⁴ Keywan Riahi, Shilpa Rao, Volker Krey, Cheolhung Cho, Vadim Chirkov, Guenther Fischer, Georg Kindermann, Nebojsa Nakicenovic, and Peter Rafaj, “RCP 8.5—A Scenario of Comparatively High Greenhouse Gas Emissions,” *Climatic Change*, Vol. 109, No. 33, 2011.

⁶⁵ R. L. Wilby and T. M. Wigley, “Downscaling General Circulation Model Output: A Review of Methods and Limitations,” *Progress in Physical Geography*, Vol. 21, No. 4, 1997, pp. 530–548.

⁶⁶ L. O. Mearns et al., *The NA-CORDEX Dataset*, Version 1.0, Boulder Colo.: NCAR Climate Data Gateway, 2017.

⁶⁷ D. Maraun, F. Wetterhall, A. M. Ireson, R. E. Chandler, E. J. Kendon, M. Widmann, S. Brienen, H. W. Rust, T. Sauter, M. Themeßl, V. K. C. Venema, K. P. Chun, C. M. Goodess, R. G. Jones, C. Onof, M. Vrac, and I. Thiele-Eich, “Precipitation Downscaling Under Climate Change: Recent Developments to Bridge the Gap Between Dynamical Models and the End User,” *Reviews of Geophysics*, Vol. 48, No. 3, September 2010.

⁶⁸ David W. Pierce, Daniel R. Cayan, and Bridget L. Thrasher, “Statistical Downscaling Using Localized Constructed Analogs (LOCA),” *Journal of Hydrometeorology*, Vol. 15, No. 6, 2014, pp. 2558–2585.

⁶⁹ John T. Abatzoglou and Timothy J. Brown, “A Comparison of Statistical Downscaling Methods Suited for Wildfire Applications,” *International Journal of Climatology*, Vol. 32, Vol. 5, April 2012, pp. 772–780.

Table 3.1. Downscaled Climate Model Datasets Utilized in This Study

Dataset	CMIP5 GCMs	RCPs	Approximate Gridded Spatial Resolution	Temporal Resolution	Downscaling Approach
BCCAv2	21	2.6, 4.5, 6.0, 8.5	12 km (7.5 miles)	Daily	Statistical
MACA	20	4.5, 8.5	4 km (2.5 miles)	Daily	Statistical
LOCA	32	4.5, 8.5	6 km (3.7 miles)	Daily	Statistical
NA-CORDEX	4	8.5	25 km (15.5 miles)	Sub-daily	Dynamical
NA-CORDEX	1	4.5	50 km (31 miles)	Sub-daily	Dynamical
NA-CORDEX	5	8.5	50 km (31 miles)	Sub-daily	Dynamical

NOTES: Only BCCAv2 RCP 4.5 and 8.5 were used in this study. MACA datasets based on METDATA calibration datasets were used. Gridded spatial resolutions across all datasets are approximate and are based on conversions from degrees to km at mid-latitudes.

These datasets are also based on rigorous data requirements, use methodologies vetted in peer-reviewed academic articles, and are viewed as trusted sources of higher-resolution future climate information. In particular, the LOCA dataset is the basis of much of the analysis in the Fourth National Climate Assessment.⁷⁰ The downscaled climate model datasets—BCCAv2, MACA, LOCA, and NA-CORDEX—are all available at a continuous temporal resolution and spatial coverage and do not come with gaps or missing data common to observation-based precipitation datasets. Of the available RCPs among these datasets, the most commonly used are RCP 8.5 and RCP 4.5, which were both included in this analysis. More information on a comparison of these datasets can be found in López-Cantú et al., 2020, and Wu et al., 2019.⁷¹⁷²

These datasets are all publicly available and were obtained for the period 1950–2099. To represent the historical period, we used the 50-year period 1950–1999 because of its alignment with Atlas 14’s historic period. Two future 50-year periods were also used: 2020–2069 and 2050–2099. These two future periods were selected after consultation with the Chesapeake Bay Program’s USWG for their relevance to regional planning and decisionmaking. Fifty-year time periods were selected because shorter time periods are suboptimal for the estimation of extremes, particularly those that are expected to occur only once in 50 or 100 years.⁷³

⁷⁰ Christopher W. Avery, David R. Reidmiller, Michael Kolian, Kenneth E. Kunkel, David Herring, Reid Sherman, William V. Sweet, Kathryn Tipton, and Christopher P. Weaver, “Data Tools and Scenario Products,” in David R. Reidmiller, Christopher W. Avery, David R. Easterling, Kenneth E. Kunkel, Kristin L. M. Lewis, Thomas K. Maycock, and Brooke C. Stewart, eds., *Impacts, Risks, and Adaptation in the United States: Fourth National Climate Assessment, Volume II*, Washington, D.C.: U.S. Global Change Research Program, 2018, pp. 1413–1430.

⁷¹ Shu Wu, Momcilo Markus, David Lorenz, James R. Angel, and Kevin Grady, “A Comparative Analysis of the Historical Accuracy of the Point Precipitation Frequency Estimates of Four Data Sets and Their Projections for the Northeastern United States,” *Water*, Vol. 11, No. 6, 2019, p. 1279.

⁷² Tania López-Cantú, Andreas F. Prein, and Constantine Samaras, “Uncertainties in Future U.S. Extreme Precipitation from Downscaled Climate Projections,” *Geophysical Research Letters*, Vol. 47, No. 9, May 16, 2020.

⁷³ Arthur T. DeGaetano and Christopher Castellano, “Selecting Time Series Length to Moderate the Impact of Nonstationarity in Extreme Rainfall Analyses,” *Journal of Applied Meteorology and Climatology*, Vol. 57, No. 10, 2018, pp. 2285–2296.

Coupled Model Intercomparison Project 6

The next evolution of the Coupled Model Intercomparison Project Phase 6 (CMIP6) is ongoing, and a limited number of CMIP6 simulations are currently available at global resolutions.^{74 75} Because these data are not yet available at higher spatial resolutions, as downscaled datasets based on CMIP6 simulations are not yet available, it was not feasible to develop IDF curve change factors based on this new generation of global climate simulations. The research team did perform a comparison of GCM-scale rainfall extremes between comparable CMIP5 and CMIP6 models and simulations. This analysis indicated that the two datasets gave similar results for the CBW and Virginia.

⁷⁴ Veronika Eyring, Sandrine Bony, Gerald A. Meehl, Catherine A. Senior, Bjorn Stevens, Ronald J. Stouffer, and Karl E. Taylor, “Overview of the Coupled Model Intercomparison Project Phase 6 (CMIP6) Experimental Design and Organization,” *Geoscientific Model Development*, Vol. 9, 2016, pp. 1937–1958.

⁷⁵ World Climate Research Program Working Group on Coupled Modeling, *CMIP6—Coupled Model Intercomparison Project Phase 6*, Livermore, Calif.: Lawrence Livermore National Laboratory, 2021.

4. Methods

This section describes the processes used to develop future IDF curves from IDF curve change factors. Our process is based on five main steps:

1. Calculate Atlas 14 IDF curves from station data for the 50-year base period 1950–1999.
2. Calculate modeled historic and future projected IDF curves from gridded downscaled climate model data for 1950–1999 (modeled historic) and 2020–2069 and 2050–2099 (future projected) for each grid cell, downscaling method, GCM, and RCP.
3. Compute change factors for each future time period (which relate future IDF curves to historic modeled IDF curves) for each grid cell, downscaling method, GCM, and RCP.
4. Quantify uncertainty in change factor calculations for each grid cell, due to statistical model fit, downscaling method, GCM, and RCP.
5. Aggregate change factors and uncertainty ranges to county scale.

In the final online data tool, change factors are accessible and available for download by county, and adjusted Atlas 14 IDF curves are also available, which apply the relevant county change factor to the station-based Atlas 14 IDF curves.

Step 1. Station-Based Atlas 14 IDF Curves

To generate station-based Atlas 14 IDF curves, the research team carried out the steps described below. The selection of methods was intended to best replicate the approaches taken to derive Atlas 14 values available from NOAA’s Precipitation Frequency Data Server (PFDS). We recreated them for this study to make sure that the methods we applied to the downscaled climate model datasets (in Step 2) were comparable to Atlas 14 and, more importantly, to assure users that the change factors developed in this study (see Step 3) could indeed be applied directly to the values obtained from Atlas 14 for the selected stations. Note that the values that are ultimately shown in the online tool are taken directly from Atlas 14.

From the observed station records that met study criteria, as described in Chapter 3, PDS were generated, using a 14-day independence to ensure that multiple events were not selected from the same storm. In Atlas 14, annual maximum series (AMS) are adjusted with an empirical transfer function to simulate PDS. Because applying this function to future rainfall series assumes that the historical relation is stationary with time, we chose to directly analyze the PDS. Using the PDS at each station, rainfall amounts corresponding to recurrence probabilities of 50 percent, 20 percent, 10 percent, 4 percent, 2 percent, and 1 percent (i.e., 2-, 5-, 10-, 25-, 50-, and 100-year storms) for one- to 24-hour durations were computed by simulating the methodology used in NOAA Atlas 14, which relies on the L-moments approach.⁷⁶ More information on Atlas

⁷⁶ The L-moments approach involves linear combinations of probability weighted moments. It is considered the state of practice and is useful for selecting the appropriate probability distribution function that best describes a given

14's methodology can be found in Bonnin et al., 2006,⁷⁷ and Perica et al., 2015.⁷⁸ The python *lmoments* package⁷⁹ was used to fit the GEV distribution to each station's PDS using the L-moments method of Hosking, 1990.⁸⁰ Although not the only valid theoretical distribution for estimating extreme rainfall probabilities, the use of the GEV has been standard practice in prior extreme rainfall analyses.⁸¹ Given the L-moments estimates for the GEV parameters, the *lmoments* library method was used to obtain the specified quantiles of the GEV distribution.

In addition, the regional L-moments procedure used in NOAA Atlas 14 Volume 10 was adapted.⁸² Although the majority of stations across the CBW and Virginia were outside of the region covered by Atlas 14 Volume 10, it is a more recent Atlas 14 volume (published in 2015) with updated methodologies. Here we assumed that the difference in methodology employed to develop Volume 10 was an improvement over the earlier implementation in Volume 2, which covers the majority of the CBW and Virginia and was published in 2006. Following the updated approach, for a given station (the base station), we selected a maximum of 20 neighboring stations, identified from the set of regional stations described in Chapter 3, to form a region around each base station. Sample L-moments were obtained for each regional station using the *lmoments* library *samlmu* routine, and a weighted average of the higher-order moments was computed based on the length of each regional station's PDS. These weighted averages, along with the base station's location parameter, were then used to obtain GEV parameters and quantiles.

Although this procedure did not exactly replicate the Atlas 14 methodology, the differences between the resulting recurrence interval rainfall amounts and those given by Atlas 14 were

rainfall frequency distribution. L-moments was first described in J. R. M. Hosking, "L-Moments: Analysis and Estimation of Distributions Using Linear Combinations of Order Statistics," *Journal of the Royal Statistical Society, Series B (Methodological)*, Vol. 52, No. 1, 1990, pp. 105–124.

⁷⁷ Geoffrey M. Bonnin, Deborah Martin, Bingzhang Lin, Tye Parzybok, Michael Yekta, and David Riley, *NOAA Atlas 14: Precipitation-Frequency Atlas of the United States, Vol. 2, Version 3.0: Delaware, District of Columbia, Illinois, Indiana, Kentucky, Maryland, New Jersey, North Carolina, Ohio, Pennsylvania, South Carolina, Tennessee, Virginia, West Virginia*, Silver Spring, Md.: U.S. Department of Commerce, National Oceanic and Atmospheric Administration, and National Weather Service, 2006.

⁷⁸ Sanja Perica, Sandra Pavlovic, Michael St. Laurent, Carl Trypaluk, Dale Unruh, Deborah Martin, and Orlan Wilhite, *NOAA Atlas 14: Precipitation-Frequency Atlas of the United States, Vol. 10, Version 3.0, Northern States: Connecticut, Maine, Massachusetts, New Hampshire, New York, Rhode Island, Vermont*, Silver Spring, Md.: U.S. Department of Commerce, National Oceanic and Atmospheric Administration, and National Weather Service, 2019.

⁷⁹ The Python *lmoments* package can be found at <https://pypi.org/project/lmoments/> (Python, "lmoments 0.2.3," webpage, February 17, 2015).

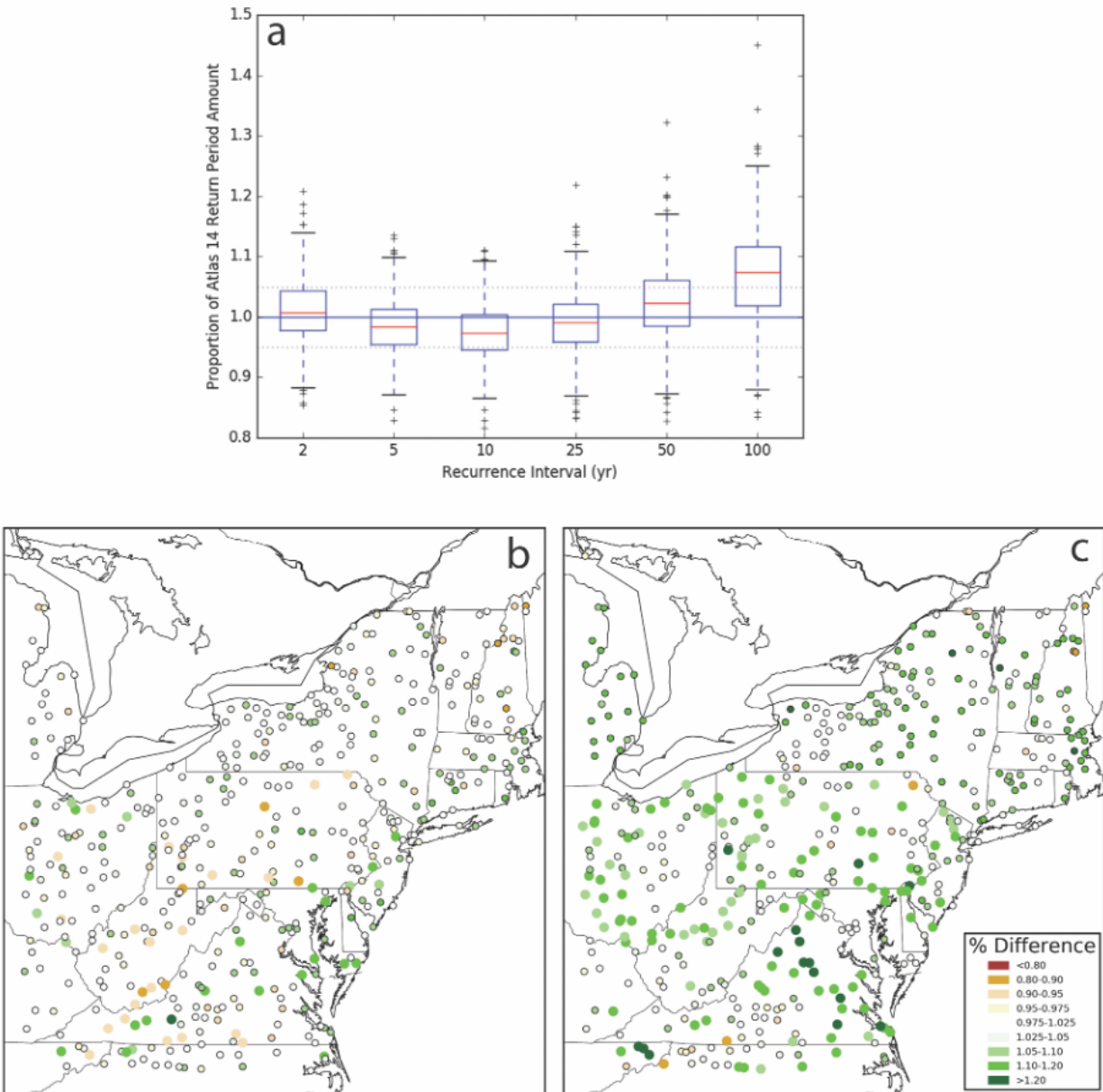
⁸⁰ J. R. M. Hosking, "L-Moments: Analysis and Estimation of Distributions Using Linear Combinations of Order Statistics," *Journal of the Royal Statistical Society, Series B (Methodological)*, Vol. 52, No. 1, 1990, pp. 105–124.

⁸¹ Simon M. Papalexiou, and Demetris Koutsoyiannis, "Battle of Extreme Value Distributions: A Global Survey on Extreme Daily Rainfall," *Water Resources Research*, Vol. 49, No. 1, January 2013, pp. 187–201.

⁸² Sanja Perica, Sandra Pavlovic, Michael St. Laurent, Carl Trypaluk, Dale Unruh, Deborah Martin, and Orlan Wilhite, *NOAA Atlas 14: Precipitation-Frequency Atlas of the United States, Vol. 10, Version 3.0, Northern States: Connecticut, Maine, Massachusetts, New Hampshire, New York, Rhode Island, Vermont*, Silver Spring, Md.: U.S. Department of Commerce, National Oceanic and Atmospheric Administration, and National Weather Service, 2019.

generally small, with most values generally falling within the published Atlas 14 confidence intervals, as shown in Figure 4.1.

Figure 4.1. Differences Between One-Day (converted to 24-hour) Atlas 14 and Project-Computed Recurrence Interval Rainfall Amounts



NOTES: 4.1a boxplots show differences for all recurrence intervals across all stations in the study domain, with the horizontal dotted lines denoting a ± 5 -percent difference between the values. Station-specific differences are shown for the two-year recurrence interval amounts in 4.1b and for the 100-year recurrence interval amounts in 4.1c. The slightly smaller station markers outlined in black indicate computed values that fall within the published Atlas 14 confidence interval.

Step 2. Downscaled Climate Model Data IDF Curves

In Step 2, the project team calculated modeled historic and future projected IDF curves from gridded downscaled climate model data for 1950–1999 (modeled historic) and 2020–2069 and 2050–2099 (future projected), with rainfall amounts corresponding to recurrence probabilities of 50 percent, 20 percent, 10 percent, 4 percent, 2 percent, and 1 percent (i.e., 2-, 5-, 10-, 25-, 50-, and 100-year storms) for 24-hour durations. IDF curve values were calculated for each grid cell, from each downscaled climate model dataset, for each GCM within a given dataset and for both RCP 4.5 and RCP 8.5. For example, this produced 32 sets of IDF curves for the above duration and recurrence intervals using LOCA’s modeled historic precipitation data for the period 1950–1999. For the two future time periods, which each have two scenarios of future greenhouse gas concentrations (RCP 4.5 and RCP 8.5), 64 sets of IDF curves were generated for each future time period (or 128 total across both time periods). This was computed for each grid cell. Across the downscaled datasets, grid cells ranged from approximately 2.5 miles by 2.5 miles in size to approximately 31 miles by 31 miles in size. Table 3.1 in Chapter 3 presents the full range of grid cell sizes.

Partial Duration Series

For each grid cell and time period, PDS were used to mimic the Atlas 14 process described above in Step 1. In addition to alignment with Atlas 14, PDS, which selects the top 50 events in a 50-year time series rather than the largest event within each year, as is the process for AMS, are able to capture extreme rainfall events regardless of their year of occurrence. AMS and PDS are both widely used approaches.^{83 84 85 86 87 88} Within each PDS, the largest 50 independent daily events were extracted, ensuring seven-day independence.

⁸³ Lauren M. Cook, Christopher J. Anderson, and Constantine Samaras, “Framework for Incorporating Downscaled Climate Output into Existing Engineering Methods: Application to Precipitation Frequency Curves,” *Journal of Infrastructure Systems*, Vol. 23, No. 4, December 2017.

⁸⁴ Arthur T. DeGaetano and Christopher M. Castellano, “Future Projections of Extreme Precipitation Intensity-Duration-Frequency Curves for Climate Adaptation Planning in New York State,” *Climate Services*, Vol. 5, January 2017, pp. 23–35.

⁸⁵ Tania López-Cantú, Andreas F. Prein, and Constantine Samaras, “Uncertainties in Future U.S. Extreme Precipitation from Downscaled Climate Projections,” *Geophysical Research Letters*, Vol. 47, No. 9, May 16, 2020.

⁸⁶ Elisa Ragno, Amir AghaKouchak, Charlotte A. Love, Linyin Cheng, Farshid Vahedifard, and Carlos H. R. Lima, “Quantifying Changes in Future Intensity-Duration-Frequency Curves Using Multimodel Ensemble Simulations,” *Water Resources Research*, Vol. 54, No. 3, 2018, pp. 1751–1764.

⁸⁷ Ranjeet Thakali, Ajay Kalra, and Sajjad Ahmad, “Understanding the Effects of Climate Change on Urban Stormwater Infrastructures in the Las Vegas Valley,” *Hydrology*, Vol. 3, No. 4, 2016, p. 34.

⁸⁸ Shu Wu, Momcilo Markus, David Lorenz, James R. Angel, and Kevin Grady, “A Comparative Analysis of the Historical Accuracy of the Point Precipitation Frequency Estimates of Four Data Sets and Their Projections for the Northeastern United States,” *Water*, Vol. 11, No. 6, 2019, p. 1279.

L-moments

From each PDS for each downscaled climate model dataset, grid cell, GCM, and RCP, the parameters of a GEV were estimated using the L-moments method to align this analysis with the Atlas 14 approach. These parameters were then used to estimate the 24-hour precipitation amounts corresponding to recurrence probabilities of 50 percent, 20 percent, 10 percent, 4 percent, 2 percent, and 1 percent (i.e., 2-, 5-, 10-, 25-, 50-, and 100-year storms). The following subsections describe additional analyses that the study team carried out to compare the L-moments method with other methods used to estimate the parameters of a GEV, as well as an analysis that compared single-location L-moments and regional L-moments for downscaled data. These two analyses support the selection of L-moments and the application of L-moments for a single grid cell, rather than using a regional approach.

Comparing L-moments with Other Methods

The study team investigated L-moments along with two other methods—the Maximum Likelihood Estimator (MLE) and the Generalized Maximum Likelihood Estimator (GMLE) methods—that have been widely used in prior work.⁸⁹ The MLE and GMLE methods have fundamentally the same objective (to maximize the log-likelihood function), but they differ in the sense that GMLE introduces a prior distribution for the shape parameter, limiting it to a physically credible interval. The R library *extRemes* was used to perform both the MLE and GMLE fit on each PDS series.⁹⁰ The Akaike Information Criterion (AIC) was then used to compare the MLE and GMLE methods. AIC has been used in previous analyses to compare extreme models.⁹¹ By comparing the AIC score in Tables 4.1 and 4.2, GMLE outperformed MLE, with approximately 25 percent of the study area performing better with MLE and 75 percent of the study area performing better with GMLE for LOCA data, according to the AIC. The GMLE method also performed better for NA-CORDEX data (see Table 4.2), with approximately 13 percent of the study area performing better with MLE and 87 percent of the study area performing better with GMLE.

⁸⁹ Eduardo S. Martins and Jerry R. Stedinger, “Generalized Maximum-Likelihood Generalized Extreme-Value Quantile Estimators for Hydrologic Data,” *Water Resources Research*, Vol. 36, No. 3, March 2000, pp. 737–744.

⁹⁰ Eric Gilleland and Richard W. Katz, “extRemes 2.0: An Extreme Value Analysis Package in R,” *Journal of Statistical Software*, Vol. 72, No. 8, 2016, pp. 1–39.

⁹¹ Hanbeen Kim, Sooyoung Kim, Hongjoon Shin, and Jun-Haeng Heo, “Appropriate Model Selection Methods for Nonstationary Generalized Extreme Value Models,” *Journal of Hydrology*, Vol. 547, April 2017, pp. 557–574.

Table 4.1. Percentages of Study Area Where MLE or GMLE Performed Better, According to the AIC for LOCA

LOCA GCM	Historical		RCP 8.5 (2020–2069)		RCP 8.5 (2050–2099)	
	MLE (%)	GMLE (%)	MLE (%)	GMLE (%)	MLE (%)	GMLE(%)
ACCESS1-0	21.17	78.83	24.89	75.11	24.74	75.26
ACCESS1-3	22.22	77.78	22.7	77.3	23.03	76.97
bcc-csm1-1	23.35	76.65	28.3	71.7	28.68	71.32
bcc-csm1-1-m	21.51	78.49	35.23	64.77	32.18	67.82
CanESM2	25.28	74.72	32.61	67.39	28.62	71.38
CCSM4	23.76	76.24	36.38	63.62	34.43	65.57
CESM1-BGC	24.67	75.33	22.57	77.43	22.46	77.54
CESM1-CAM5	25.01	74.99	26.14	73.86	23.33	76.67
CMCC-CM	21.56	78.44	25.35	74.65	17.56	82.44
CMCC-CMS	25.81	74.19	22.28	77.72	22.17	77.83
CNRM-CM5	22.32	77.68	29.01	70.99	23.11	76.89
CSIRO-Mk3-6-0	25.82	74.18	24.63	75.37	26.58	73.42
EC-EARTH	26.01	73.99	27.19	72.81	23.43	76.57
FGOALS-g2	22.6	77.4	23.52	76.48	26.41	73.59
GFDL-CM3	26.73	73.27	24.93	75.07	25.26	74.74
GFDL-ESM2G	25.99	74.01	24.15	75.85	25.37	74.63
GFDL-ESM2M	23.97	76.03	28.02	71.98	30.57	69.43
GISS-E2-R	24.5	75.5	21.99	78.01	23.9	76.1
HadGEM2-AO	22.74	77.26	22.55	77.45	24.03	75.97
HadGEM2-CC	22.72	77.28	25.39	74.61	22.09	74.19
HadGEM2-ES	23.03	76.97	23.53	76.47	22.8	77.2
inmcm4	23.61	76.39	28.07	71.93	25.07	74.93
IPSL-CM5A-LR	24.88	75.12	22.4	77.6	25.36	74.64
IPSL-CM5A-MR	21.66	78.34	21.6	78.4	19.5	80.5
MIROC-ESM	21.61	78.39	23.4	76.6	27.49	72.51
MIROC-ESM-CHEM	24.47	75.53	25.63	74.37	26.58	73.42
MIROC5	23.72	76.28	22.32	77.68	24.9	75.1
MPI-ESM-LR	23.69	76.31	25.57	74.43	21.16	78.84
MPI-ESM-MR	22.5	77.5	29.82	70.18	30.17	69.83
MRI-CGCM3	24.11	75.89	24.4	75.6	28.75	71.25
NorESM1-M	27.95	72.05	27.26	72.74	32.63	67.37
Average	23.83	76.16	25.87	74.13	25.56	74.32

NOTES: We compared the performance of MLE and GMLE methods in terms of AIC to estimate the parameters of the GEV distribution for each LOCA model and period for RCP 8.5.

Table 4.2. Percentages of Study Area Where MLE or GMLE Performed Better, According to the AIC for NA-CORDEX (50 km)

NA-CORDEX (50 km) GCM	Historical		RCP 8.5 (2020–2069)		RCP 8.5 (2050–2099)	
	MLE (%)	GMLE (%)	MLE (%)	GMLE (%)	MLE (%)	GMLE (%)
CanESM2.CanRCM4	13.54	86.46	15.1	84.9	12.24	87.76
CanESM2.CRCM5-UQAM	5.99	94.01	7.03	92.97	7.55	92.45
EC-EARTH.HIRHAM5	11.46	88.54	8.33	91.67	13.54	86.46
EC-EARTH.RCA4	18.23	81.77	10.16	89.84	17.45	82.55
GEMatm-Can.CRCM5-UQAM	15.36	84.64	14.58	85.42	5.73	94.27
GEMatm-MPI.CRCM5-UQAM	14.32	85.68	11.2	88.8	16.93	83.07
GFDL-ESM2M.RegCM4	14.58	85.42	17.19	82.81	11.2	88.8
GFDL-ESM2M.WRF	10.42	89.58	9.9	90.1	20.57	79.43
HadGEM2-ES.RegCM4	16.93	83.07	8.85	91.15	6.51	93.49
HadGEM2-ES.WRF	10.68	89.32	10.68	89.32	8.85	91.15
MPI-ESM-LR.CRCM5-UQAM	8.07	91.93	15.36	84.64	14.58	85.42
MPI-ESM-LR.RegCM4	12.76	87.24	18.75	81.25	12.24	87.76
MPI-ESM-LR.WRF	11.72	88.28	13.54	86.46	11.72	88.28
MPI-ESM-MR.CRCM5-UQAM	13.8	86.2	13.02	86.98	16.41	83.59
Average	12.70	87.30	12.40	87.59	12.53	87.46

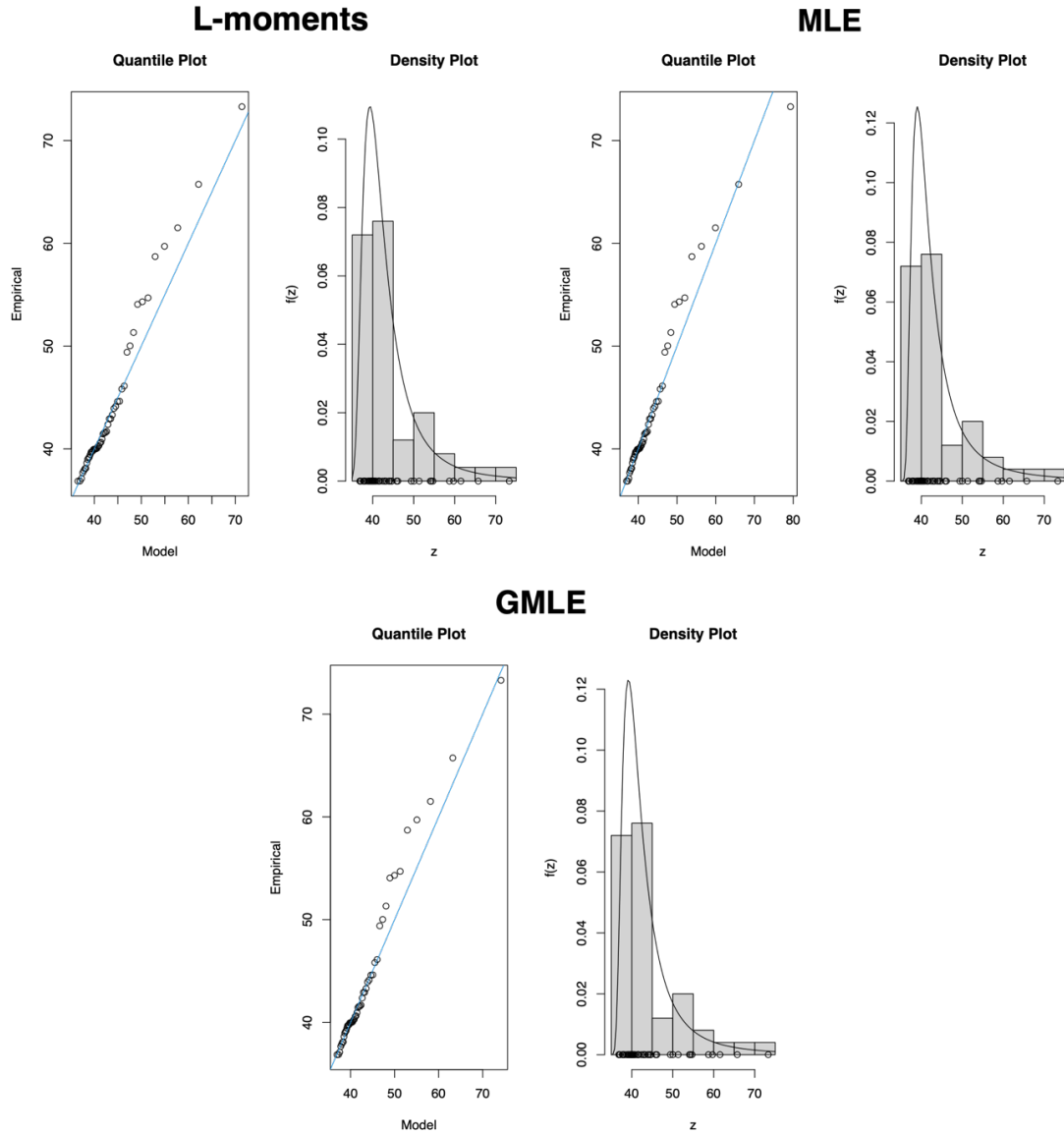
NOTES: We compared the performance of MLE and GMLE methods in terms of AIC to estimate the parameters of the GEV distribution for each NA-CORDEX model and period for RCP 8.5.

The research team also performed a visual comparison using quantile and density plots of the three fitting techniques. An example of the fit for each method is shown in Figure 4.2 for a grid cell near Harrisburg, Pennsylvania. In many cases, the L-moments, MLE, and GMLE methods led to similar parameters. Although the GMLE was preferred to MLE, as shown above, the team opted to use the L-moments method given that the GMLE method requires prior assumptions about the shape parameter and that L-moments aligns with Atlas 14. Furthermore, prior studies on rainfall extremes recommend using L-moments when the number of years on record is greater than or equal to 50, which is the case in this analysis.^{92 93} Finally, the plots in Figure 4.2 also indicate that the choice of L-moments is similar to those of GMLE and MLE and that alignment with Atlas 14 will not necessarily lead to a loss in the goodness of fit.

⁹² Benjamin Poschod, Ralf Ludwig, and Jana Sillmann, “Ten-Year Return Levels of Sub-Daily Extreme Precipitation over Europe,” *Earth System Science Data*, Vol. 13, No. 3, 2021, pp. 983–1003.

⁹³ Viatcheslav V. Kharin and Francis W. Zwiers, “Changes in the Extremes in an Ensemble of Transient Climate Simulations with a Coupled Atmosphere–Ocean GCM,” *Journal of Climate*, Vol. 13, No. 21, 2000, pp. 3760–3788.

Figure 4.2. Quantile and Density Plots of the Fit GEV Distribution Using L-Moments, MLE, and GMLE



NOTES: These plots are for a grid cell near Harrisburg, Pennsylvania, for PDS (2050–2099) extracted from the LOCA downscaled ACCESS1-0 model for RCP 8.5.

The goodness of fit was further assessed across these three methods by applying the two-tailed Kolmogorov-Smirnov test,^{94 95} which suggested that L-moments performed well in estimated GEV parameters compared with the other two methods. This is in general agreement with other studies, concluding that the L-moments method results in robust estimates of the GEV parameters.⁹⁶

Comparing with Regional L-moments

The Atlas 14 approach utilizes regional L-moments, which take into account neighboring stations when fitting a GEV for a given station. In the case of downscaled gridded data, this would suggest incorporating neighboring grid cell values when fitting the GEV for a grid cell’s PDS. The study team investigated whether adding regional L-moments would affect the change factors (change factors are described in Step 3) before determining whether the application of regional L-moments was justified in this study. Regional L-moments and single grid L-moments were calculated for all NA-CORDEX GCMs for RCP 8.5 for 2050–2099. The regional L-moments calculation incorporates the 20 closest grid points to define higher-order moments. For this analysis, we performed a straight fit to the grid point values with no resampling.

Table 4.3 and Figure 4.3 show the ratio between regional L-moments to a single-grid L-moment approach, where 1 indicates the same value and 1.01 suggests a 1-percent higher change factor when regional L-moments are used. The values in Table 4.3 and Figure 4.3 suggest that the single grid L-moments approach is on average the same as the regional L-moments and that the regional approach is not warranted. Table 4.3 shows average values, while Figure 4.3 shows ratios across all grid points and NA-CORDEX GCMs (there are about 11,000 points in each box plot).

Table 4.3. Average Ratio of Change Factors Calculated with Regional L-moments to Single-Grid L-Moments for NA-CORDEX (RCP 8.5, 2050–2099), for Each Recurrence Interval

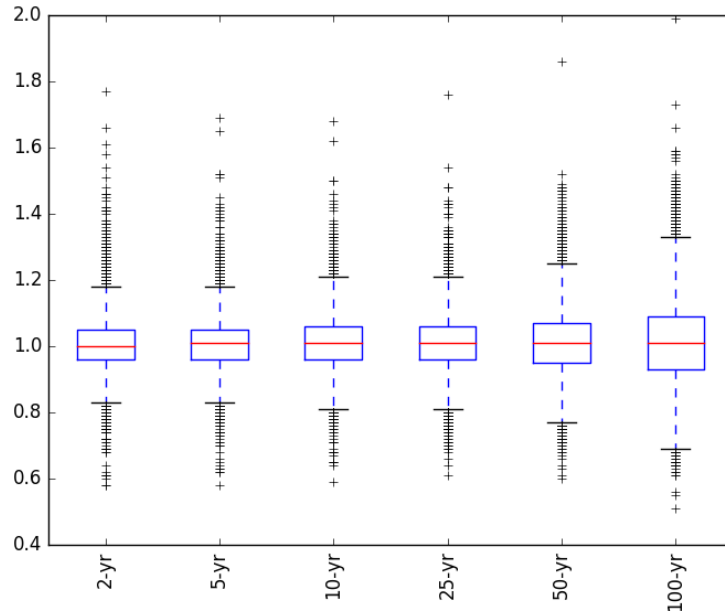
	2-Year	5-Year	10-Year	25-Year	50-Year	100-Year
Mean	1.00	1.01	1.01	1.01	1.01	1.01
Median	1.00	1.01	1.01	1.01	1.01	1.00
25th percentile	0.98	0.98	0.98	0.98	0.98	0.97
75th percentile	1.03	1.03	1.03	1.03	1.04	1.04

⁹⁴ Lauren M. Cook, Seth McGinnis, and Constantine Samaras, “The Effect of Modeling Choices on Updating Intensity-Duration-Frequency Curves and Stormwater Infrastructure Designs for Climate Change,” *Climatic Change*, Vol. 159, No. 2, 2020, pp. 289–308.

⁹⁵ Hongjoon Shin, Younghun Jung, Changsam Jeong, and Jun-Haeng Heo, “Assessment of Modified Anderson–Darling Test Statistics for the Generalized Extreme Value and Generalized Logistic Distributions,” *Stochastic Environmental Research and Risk Assessment*, Vol. 26, No. 1, 2012, pp. 105–114.

⁹⁶ Benjamin Poschlod, Ralf Ludwig, and Jana Sillmann, “Ten-Year Return Levels of Sub-Daily Extreme Precipitation over Europe,” *Earth System Science Data*, Vol. 13, No. 3, 2021, pp. 983–1003.

Figure 4.3. Ratio of Change Factors Calculated with Regional L-moments to Single-Grid L-Moments for NA-CORDEX (RCP 8.5, 2050–2099) (y axis), for Each Recurrence Interval (x axis)



NOTE: The y axis shows the ratio of the change factor calculated with the regional L-moments approach compared with the single-grid L-moment.

Step 3. Climate Change–Informed IDF Curve Change Factors

After the 24-hour rainfall depths were calculated for the 2-, 5-, 10-, 25-, 50-, and 100-year rainfall events for the historic period and the two future periods in Step 2, the research team used these three values to calculate IDF curve change factors. Change factors represent the change signal seen between historic and future periods in climate projections.⁹⁷ Change factors are calculated based on the quantile delta method (QDM), in which changes between historic and future values are estimated separately by *quantiles*: discrete segments within a probability distribution.⁹⁸ IDF curves are already calculated based on recurrence probabilities of 50 percent, 20 percent, 10 percent, 4 percent, 2 percent, and 1 percent, so the QDM or change factors are therefore a ratio of the future time period 24-hour rainfall depth for a given recurrence interval to the historic modeled 24-hour rainfall depth for the same recurrence interval. Equation 4.1 shows the change factor calculation for a two-year rainfall event for the 2020–2069 future time period.

⁹⁷ Tania López-Cantú, Andreas F. Prein, and Constantine Samaras, “Uncertainties in Future U.S. Extreme Precipitation from Downscaled Climate Projections,” *Geophysical Research Letters*, Vol. 47, No. 9, May 16, 2020.

⁹⁸ Alex J. Cannon, Stephen R. Sobie, and Trevor Q. Murdock, “Bias Correction of GCM Precipitation by Quantile Mapping: How Well Do Methods Preserve Changes in Quantiles and Extremes?” *Journal of Climate*, Vol. 28, No. 17, 2015, pp. 6938–6959.

⁹⁹ Harris Switzman, Tara Razavi, Serge Traore, Paulin Coulibaly, Donald H. Burn, John Henderson, Edmundo Fausto, and Ryan Ness, “Variability of Future Extreme Rainfall Statistics: Comparison of Multiple IDF Projections,” *Journal of Hydrologic Engineering*, Vol. 22, No. 10, October 2017.

$$\text{Change Factor}_{2020-2069} = \frac{2\text{yr},24\text{hr rainfall depth}_{2020-2069}}{2\text{yr},24\text{hr rainfall depth}_{1950-1999}} \quad (4.1)$$

The change factor calculation was carried out for each recurrence interval, for each grid cell, each future time period (both 2020–2069 and 2050–2099), each downscaled climate model dataset, each GCM, and each RCP. This resulted in, for example, 24 change factors per grid cell for NA-CORDEX and 128 change factors per grid cell for LOCA for a given recurrence interval. Because change factors are essentially a scalar between the historic period and the future period of interest, with the same baseline period as Atlas 14 and the underlying data derived in the same way as Atlas 14, these change factors can be directly multiplied by the Atlas 14 values for the respective recurrence interval to obtain the climate-adjusted IDF curves for a given station. Importantly, this study recommends applying change factors calculated based on 24-hour rainfall depths across all rainfall durations in Atlas 14. This procedure and the correct and incorrect use of change factors are described in more detail in Chapter 5.

This approach was selected for a number of reasons. First, change factors are widely used and conceptually simple to understand, dating back as early as 1989 to a pioneering study of climate change impacts on the stormwater system in Lund, Sweden.^{100 101} Second, the resolution of the downscaled climate model datasets did not match the station scale at which climate adjustments were to be applied. The change factor method allowed the study team to overcome this spatial mismatch by translating the estimated changes in IDF curves calculated from downscaled climate model output to Atlas 14 values.^{102 103} Third, change factors avoid some of the complexities of other methodologies, such as spurious trends from the application of parametric relationships between simulated and observed data.^{104 105} Finally, the change factor approach eliminates biases that a GCM or downscaling method might introduce by taking the

¹⁰⁰ Janusz Niemczynowicz, “Impact of the Greenhouse Effect on Sewerage Systems—Lund Case Study,” *Hydrological Sciences Journal*, Vol. 34, No. 6, 1989, pp. 651–666.

¹⁰¹ J. Olsson, K. Berggren, M. Olofsson, and M. Viklander, “Applying Climate Model Precipitation Scenarios for Urban Hydrological Assessment: A Case Study in Kalmar City, Sweden,” *Atmospheric Research*, 7th International Workshop on Precipitation in Urban Areas, Vol. 92, No. 3, May 2009, pp. 364–375.

¹⁰² Alex J. Cannon, Stephen R. Sobie, and Trevor Q. Murdock, “Bias Correction of GCM Precipitation by Quantile Mapping: How Well Do Methods Preserve Changes in Quantiles and Extremes?” *Journal of Climate*, Vol. 28, No. 17, 2015, pp. 6938–6959.

¹⁰³ J. Olsson, K. Berggren, M. Olofsson, and M. Viklander, “Applying Climate Model Precipitation Scenarios for Urban Hydrological Assessment: A Case Study in Kalmar City, Sweden,” *Atmospheric Research*, 7th International Workshop on Precipitation in Urban Areas, Vol. 92, No. 3, May 2009, pp. 364–375.

¹⁰⁴ Chun-Chao Kuo, Thian Yew Gan, and Mesgana Seyoum, “Potential Impact of Climate Change on Intensity Duration Frequency Curves of Central Alberta,” *Climatic Change*, Vol. 130, No. 2, 2015, pp. 115–129.

¹⁰⁵ Roshan K. Srivastav, Andre Schardong, and Slobodan P. Simonovic, “Equidistance Quantile Matching Method for Updating IDF Curves Under Climate Change,” *Water Resources Management*, Vol. 28, No. 9, 2014, pp. 2539–2562.

ratio between historical and future projected values for a given GCM or downscaling method, rather than applying projected values directly, which would preserve these biases.¹⁰⁶

We also make the assumption in this study that change factors calculated based on 24-hour modeled historic and simulated future values are applicable across all duration events. This assumption allows us to create a range of change factors that contain information across the downscaled climate model datasets. LOCA, MACA, and BCCAv2 downscaled simulations are only available at a daily resolution, and although temporal disaggregation methods exist (e.g., Segond et al., 2006), a wide-coverage network of high-quality long hourly rainfall data within the study area is required.¹⁰⁷ Such a requirement is not evenly available across the CBW or Virginia. Furthermore, more research is needed to better understand and detect changes in hourly extremes compared with daily extremes in GCMs,¹⁰⁸ which also suggests that change factors based on 24-hour IDF curve values might be leveraging the best available science at the time of analysis. Finally, previous analysis of sub-daily and daily rainfall extremes show that for selected cities in the broader region (e.g., Pittsburgh, Baltimore, and New York), one-hour and 24-hour duration change factors are virtually equal.¹⁰⁹

In addition, the team tested this assumption with an analysis of sub-daily change factors derived from hourly simulations from the NA-CORDEX archive. The number of sub-daily NA-CORDEX downscaled simulations available for each RCP is shown in Chapter 3, Table 3.1. Figure 4.4 shows the distribution of change factors at grid cells within the study area. When compared with the same analysis of 24-hour data, this analysis revealed that the variability in the one-hour change factors at the study region was generally of the same magnitude as daily change factors. In a few cases in Figure 4.4, the large variability could be due to various factors, including the small number of hourly downscaled simulations to analyze. Additional research is needed to understand the advantages, disadvantages, and uncertainties introduced into sub-hourly disaggregation for future climate projections used for decisionmaking.

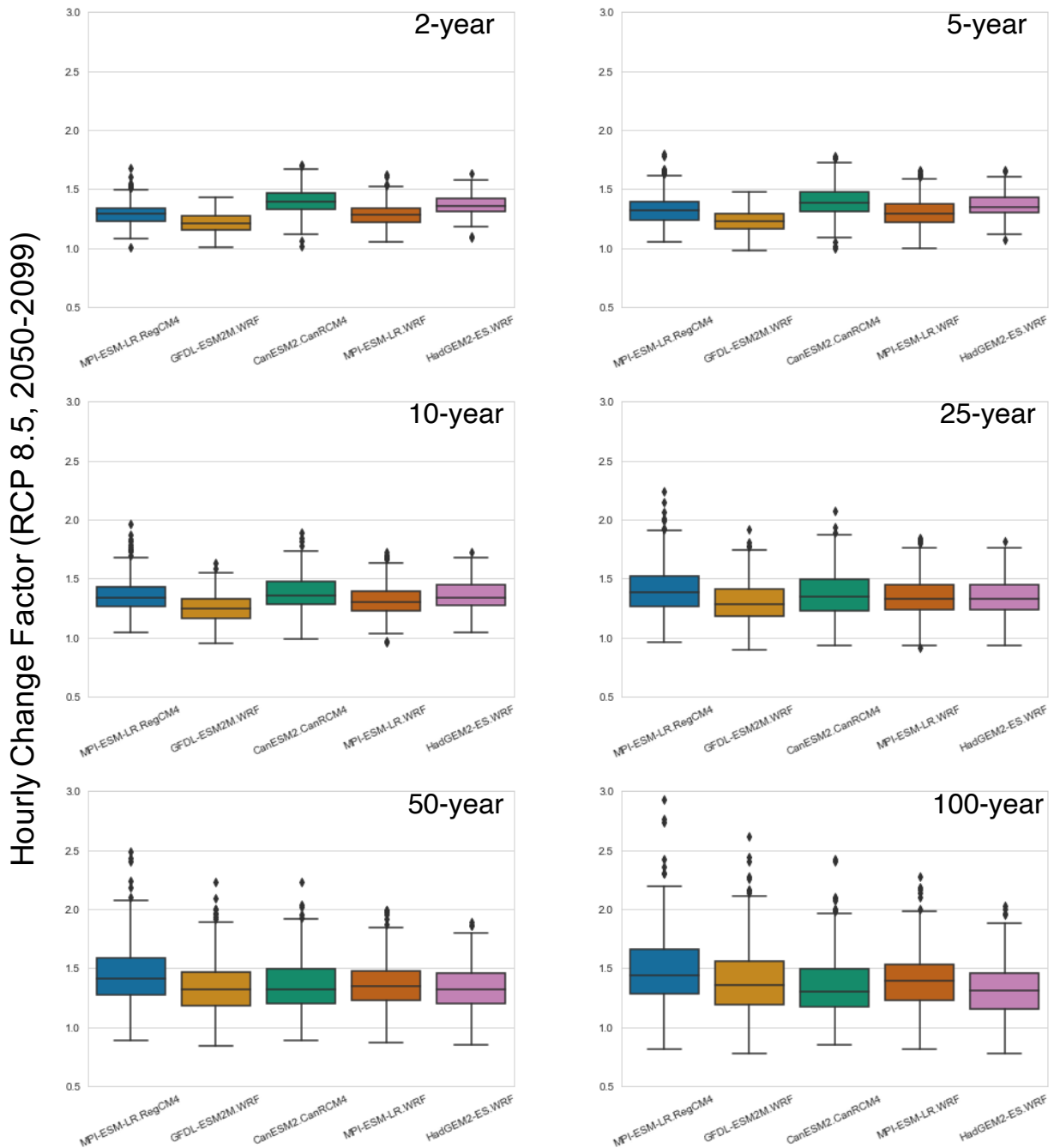
¹⁰⁶ Claudia Teutschbein and Jan Seibert, “Bias Correction of Regional Climate Model Simulations for Hydrological Climate-Change Impact Studies: Review and Evaluation of Different Methods,” *Journal of Hydrology*, Vol. 456–457, August 16, 2012, pp. 12–29.

¹⁰⁷ M.-L. Segond, C. Onof, and H. S. Wheater, “Spatial–Temporal Disaggregation of Daily Rainfall from a Generalized Linear Model,” *Journal of Hydrology*, Vol. 331, Nos. 3–4, December 2006, pp. 674–689.

¹⁰⁸ Hayley J. Fowler, Haider Ali, Richard P. Allan, Nikolina Ban, Renaud Barbero, Peter Berg, Stephen Blenkinsop, Nalan Senol Cabi, Steven Chan, Murray Dale, Robert J. H. Dunn, Marie Ekström, Jason P. Evans, Giorgia Fossier, Brian Golding, Selma B. Guerreiro, Gabriele C. Hegerl, Abdullah Kahraman, Elizabeth J. Kendon, Geert Lenderink, Elizabeth Lewis, Xiaofeng Li, Paul A. O’Gorman, Harriet G. Orr, Katy L. Peat, Andreas F. Prein, David Pritchard, Christoph Schär, Ashish Sharma, Peter A. Stott, Roberto Villalobos-Herrera, Gabriele Villarini, Conrad Wasko, Michael F. Wehner, Seth Westra, and Anna Whitford, “Towards Advancing Scientific Knowledge of Climate Change Impacts on Short-Duration Rainfall Extremes,” *Philosophical Transactions of the Royal Society A: Mathematical, Physical and Engineering Sciences*, Vol. 379, No. 2195, April 2021.

¹⁰⁹ Lauren M. Cook, Seth McGinnis, and Constantine Samaras, “The Effect of Modeling Choices on Updating Intensity-Duration-Frequency Curves and Stormwater Infrastructure Designs for Climate Change,” *Climatic Change*, Vol. 159, No. 2, 2020, pp. 289–308.

Figure 4.4. Analysis of Sub-Daily NA-CORDEX (50 km) Change Factors for RCP 8.5 (2050–2099)



NOTE: Boxplots show the distribution of change factors at grid cells within the study area.

Finally, once change factors were calculated across the study region, we examined them for each of the downscaled climate model datasets. Because only one GCM was common across the four datasets—the CanESM2 model—this analysis was limited to a comparison of the CanESM2 change factors across all models. This comparison revealed consistent results in terms of regional

patterns and the directionality of change factors across LOCA and NA-CORDEX but divergent patterns across MACA and BCCAv2. For the latter two datasets, the calculated changes were also not consistent with recent regional trends. A similar analysis was performed in López-Cantú, Prein, and Samaras, 2020, that confirmed these findings for MACA and BCCAv2 (see Figures S11, S12 and S13 in the Supplementary Information in that document).¹¹⁰ As a result, the study team elected to pull MACA and BCCAv2 out of the final datasets produced by this study.

Step 4. Uncertainty Bounds for IDF Curve Change Factors

Uncertainty in IDF curve change factors comes from a number of sources, such as those inherent in the datasets and their underlying models and assumptions, as well as from the methodologies used in this study. To characterize the uncertainty in the IDF curve change factors generated in this study, we quantified the range of possible IDF curve values resulting from variability in values caused by (1) the L-moments statistical fitting technique, (2) the downscaling methods, (3) the GCMs, and (4) the future greenhouse gas concentration scenario (RCP).

To quantify the range of possible IDF curve values resulting from the estimation of rainfall depths from the L-moments technique, a parametric bootstrapping approach was employed. Because no single draw from a probability distribution will likely be exactly the same, resampling methods, such as bootstrapping, are used to develop confidence intervals around values estimated from a probability distribution.¹¹¹ For each grid cell, GCM, RCP, and downscaled climate model dataset, the fitted GEV distribution was sampled 100 times to obtain 100 estimates of a given rainfall depth for a given recurrence interval and time period. For each bootstrap run, change factors were calculated, resulting in a range of change factors for each recurrence interval, grid cell, GCM, RCP, and downscaled climate model dataset. This process was carried out as part of Steps 2 and 3 but is noted here because of its relevance to uncertainty.

Because RCPs represent different scenarios about our future atmospheric greenhouse gas concentrations, the selection of an RCP will change the IDF curves and thus the change factors produced. Similarly, the underlying processes and assumptions within the suite of GCMs downscaled in the four downscaled datasets will affect the results even with their standardized set of inputs as a part of CMIP5. The downscaling approaches used across NA-CORDEX and LOCA mean that more-localized estimates of precipitation are obtained with different dynamical or statistical approaches, also influencing the IDF curve values and subsequent change factors.¹¹² Rather than average or simplify these data, this full range of precipitation estimates constitutes a

¹¹⁰ Tania López-Cantú, Andreas F. Prein, and Constantine Samaras, “Uncertainties in Future U.S. Extreme Precipitation from Downscaled Climate Projections,” *Geophysical Research Letters*, Vol. 47, No. 9, May 16, 2020.

¹¹¹ Dennis R. Helsel, Robert M. Hirsch, Karen R. Ryberg, Stacey A. Archfield, and Edward J. Gilroy, *Statistical Methods in Water Resources: U.S. Geological Survey Techniques and Methods*, Book 4, Chapter A3, Reston, Va.: U.S. Geological Survey, 2020.

¹¹² Tania López-Cantú, Andreas F. Prein, and Constantine Samaras, “Uncertainties in Future U.S. Extreme Precipitation from Downscaled Climate Projections,” *Geophysical Research Letters*, Vol. 47, No. 9, May 16, 2020.

rich source of information about our future climate. To characterize the range in change factors caused by climate model data (RCP, GCM, and downscaling approach), change factors were calculated for each downscaled dataset, GCM, and RCP, as noted throughout Steps 2 and 3.

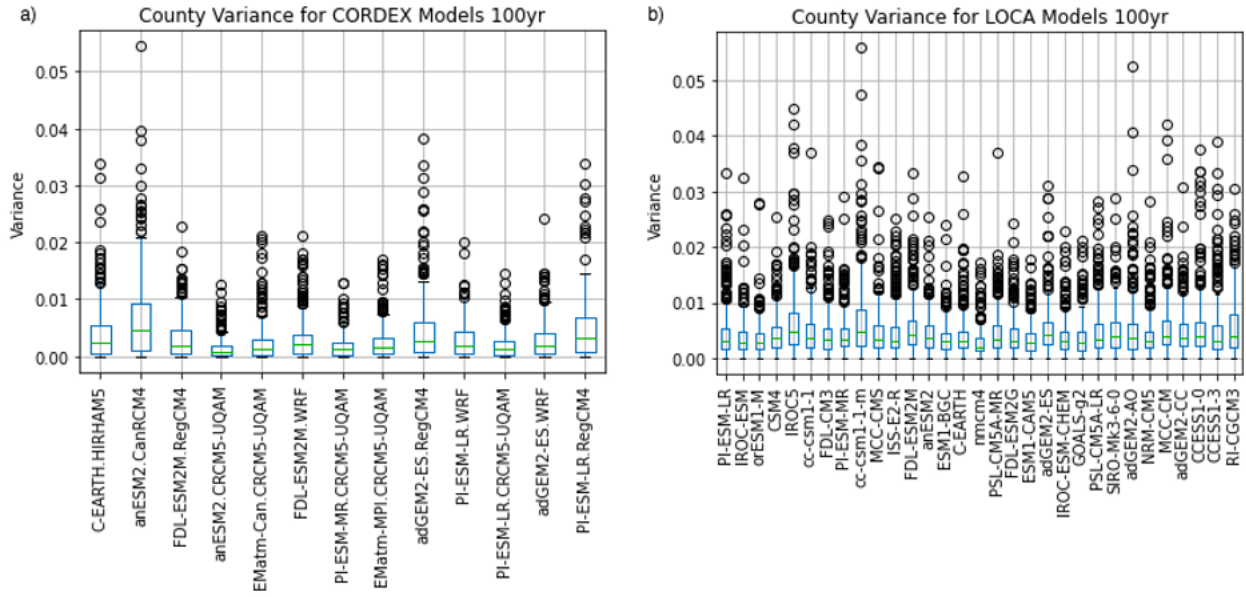
To determine the full confidence interval, or uncertainty range, for IDF curve change factors, summary statistics were run on the ensemble of change factors calculated across the bootstrapping runs, GCMs, and downscaling approaches. The median, 25th-percentile, 75th-percentile, 10th-percentile, and 90th-percentile change factors across this ensemble were recorded for each grid cell, RCP, and recurrence interval. As described in Chapter 5, users of the data tool are able to select their RCP and recurrence interval of interest, so confidence intervals were calculated for each grid cell, RCP, and recurrence interval combination.

Step 5. County-Level Change Factors with Uncertainty Bounds

In early conversations with the Chesapeake Bay Program's USWG, members expressed a strong interest in county-level, rather than gridded, change factors. To produce these data, the study team performed an area-weighted average of the change factors for the grid cells or portions of grid cells within county boundaries. These area-weighted averages were performed for all counties crossing the CBW boundaries, as well as all counties in the Commonwealth of Virginia. Area-weighted averages were calculated for the median, 25th-percentile, 75th-percentile, 10th-percentile, and 90th-percentile change factors for each county, RCP, and recurrence interval.

The study team also performed an analysis on uncertainty resulting from applying this aggregation method. The research team calculated the variance in the grid cell change factors used to calculate the county averages to see whether this county-level variance was higher or lower than the uncertainty bounds already computed in Step 4. The variance across grid cell change factors within each county is shown in Figure 4.5. A high variance would suggest that one part of a county could have significantly different change factor than another part of that county. However, the results showed a low variance among grid cell change factors within counties, and the suggested county-level change factors are appropriate. Furthermore, by comparing the values in Figure 4.5 with the uncertainty bounds from Step 4, we found that the contribution to uncertainty was negligible, and, therefore, we did not adjust the change factor confidence intervals.

Figure 4.5. Variance in Grid Cell Change Factors by County Across Study Region for the 100-Year Recurrence Interval



NOTES: Boxplots show variance for NA-CORDEX models (in 5a) and LOCA models (5b) for the 100-year recurrence interval. The grid cells used to calculate the county variance were the same grid cells used to calculate the county area-weighted average.

5. Results and Data Tool

The primary results of this study are projected IDF curves, based on IDF curve change factors, for two future time periods (2020–2069 and 2050–2099) and two future greenhouse gas concentration scenarios (RCP 4.5 and RCP 8.5). IDF curve change factors are calculated at the county level for each time period, RCP, and recurrence interval. These factors are applied to generate projected IDF curves at 2-, 5-, 10-, 25-, 50-, and 100-year recurrence intervals for 1-, 2-, 3-, 6-, 12-, 18-, and 24-hour durations for stations with adequate records across the CBW and Virginia. Table 5.1 depicts the median county-level change factors across the study region. This table underscores that, according to the data and methods used in this study, regardless of recurrence interval, scenario, time period, or downscaling method, the CBW and Virginia will see increases in extreme precipitation compared with 1950–1999. On average, these changes will range from an 8-percent increase to a 20-percent increase. Table 5.1 shows that RCP 8.5, which represents a future with higher atmospheric greenhouse gas concentrations, predicts higher change factors across the region, particularly by the second half of the 21st century. Results also show that NA-CORDEX, which uses a dynamical method to downscale GCM data, estimates slightly higher change factors than LOCA. Furthermore, these regional averages indicate greater change factors for the lower-frequency but higher-magnitude events.

Table 5.1. Study Area Averaged Ensemble Median Change Factors for Each Recurrence Interval, RCP, Future Period, and Downscaled Climate Model Dataset

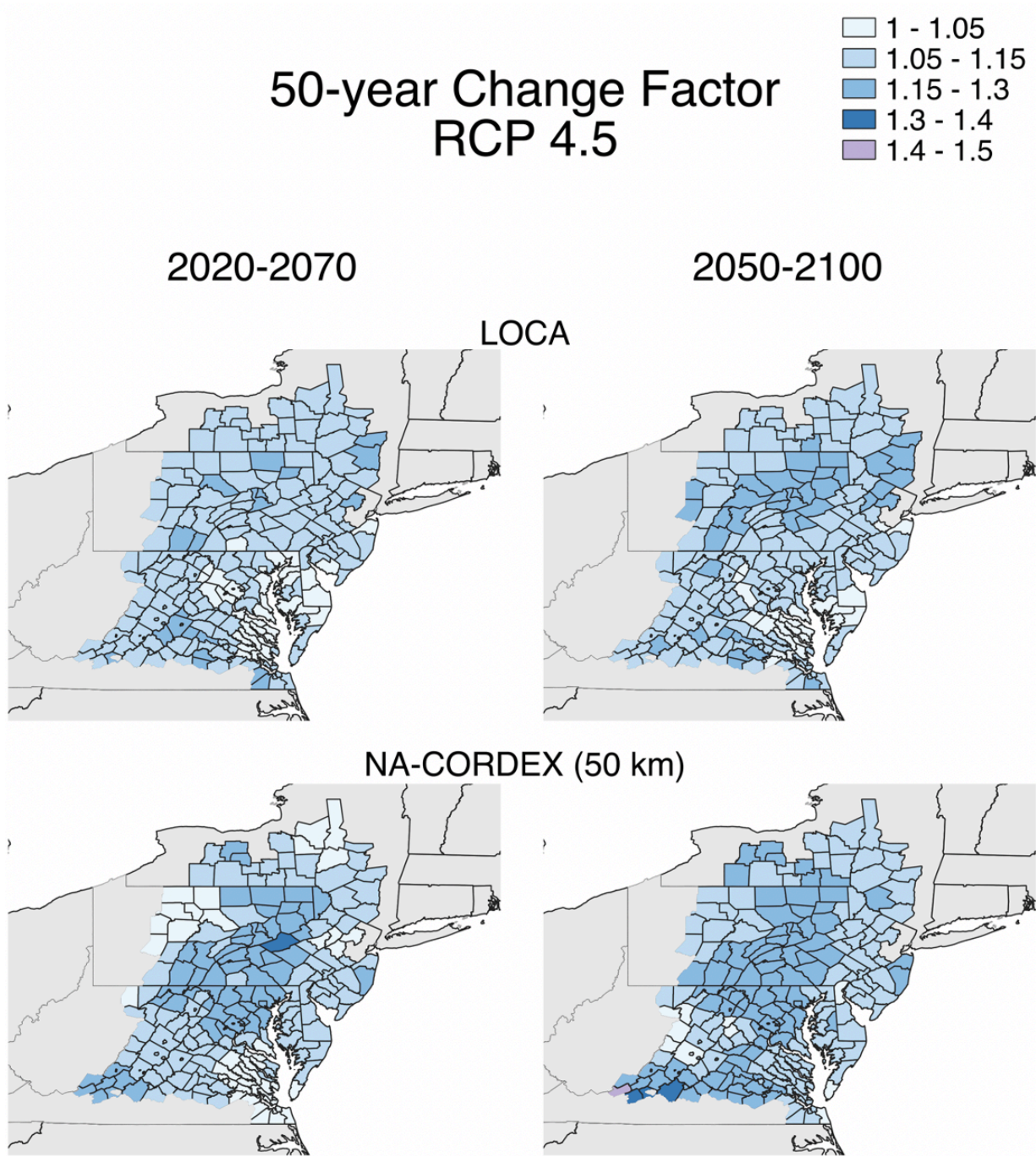
			2-Year	5-Year	10-Year	25-Year	50-Year	100-Year
LOCA	RCP 4.5	2020–2069	1.08	1.08	1.09	1.09	1.10	1.10
		2050–2099	1.11	1.11	1.11	1.12	1.12	1.13
	RCP 8.5	2020–2069	1.10	1.10	1.10	1.11	1.11	1.11
		2050–2099	1.18	1.18	1.18	1.18	1.18	1.18
NA-CORDEX	RCP 4.5	2020–2069	1.10	1.10	1.10	1.11	1.11	1.12
		2050–2099	1.13	1.14	1.14	1.15	1.15	1.16
	RCP 8.5	2020–2069	1.11	1.12	1.12	1.13	1.13	1.14
		2050–2099	1.18	1.19	1.20	1.20	1.20	1.20

Figures 5.1 through 5.4 show the spatial pattern of these change factors by RCP and dataset for both time periods for CBW (Figures 5.1 and 5.2) and Virginia (Figures 5.3 and 5.4). From all four figures, it is evident that there is no clear spatial pattern that is consistent across RCPs, time

periods, or models, underscoring the importance of considering multiple climate model datasets when attempting to characterize future changes. There are a few notable regional patterns within a dataset, including, for example, larger change factors in RCP 4.5 in Western Virginia, particularly in the second time period. Interestingly, in RCP 8.5, this portion of Virginia shows higher change factors in the first time period and a slightly lower increase in IDF curve values for the later time period. Additionally, except for a few similar outliers, the general trends of Table 5.1 hold across the county-level change factors, rather than the regional median change factors—change factors generally increase between RCP 4.5 and 8.5 and from 2020–2069 to 2050–2099.

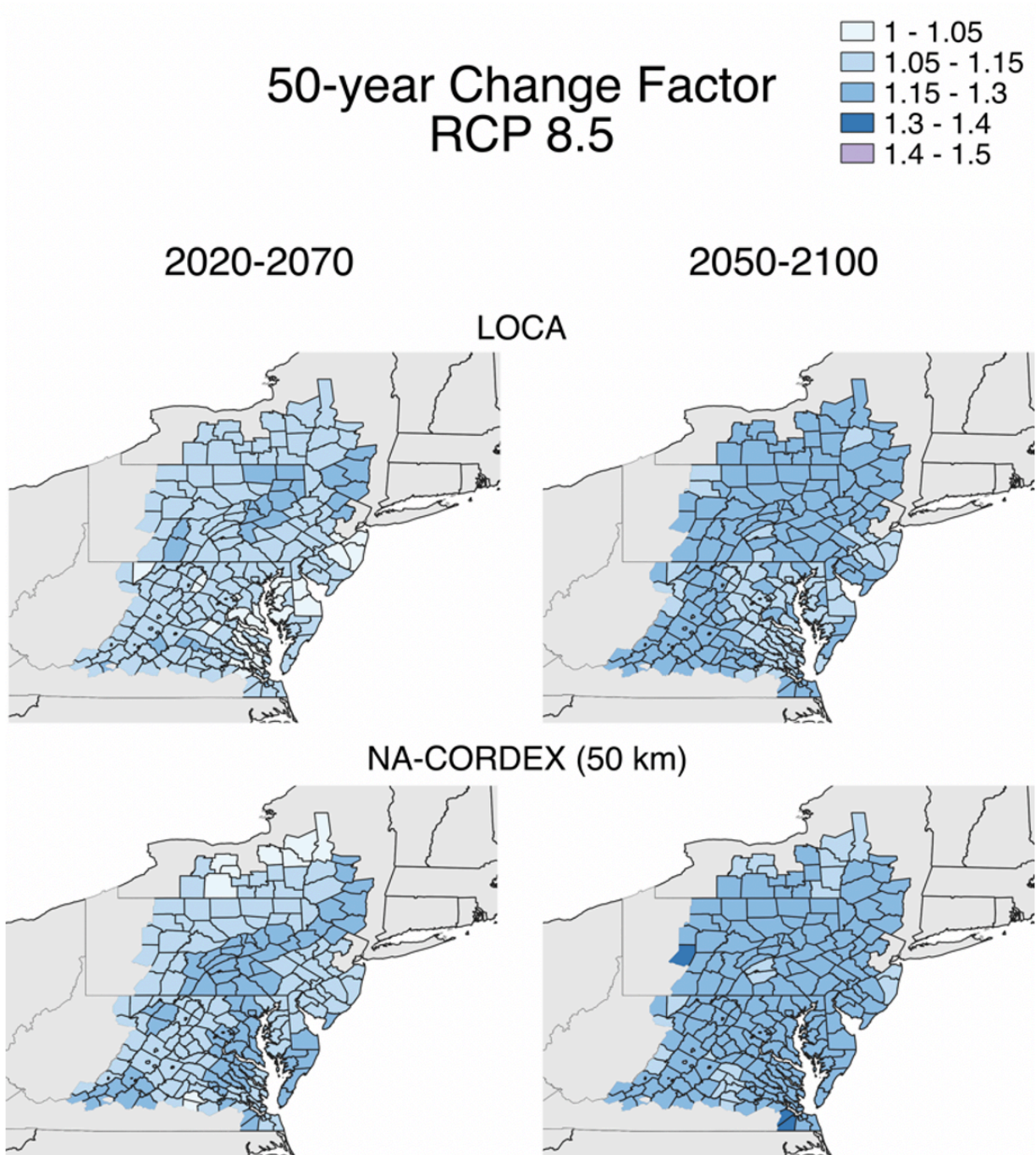
Individual station-based and county-level results, including their uncertainty ranges, are available in the online tool, and results can be viewed and analyzed by users via the interactive options. This tool is described in the following chapter.

Figure 5.1. County-Level Change Factors for the CBW Projected by the Ensemble Median of All GCMs in Each Dataset for Both Future Periods Under RCP 4.5



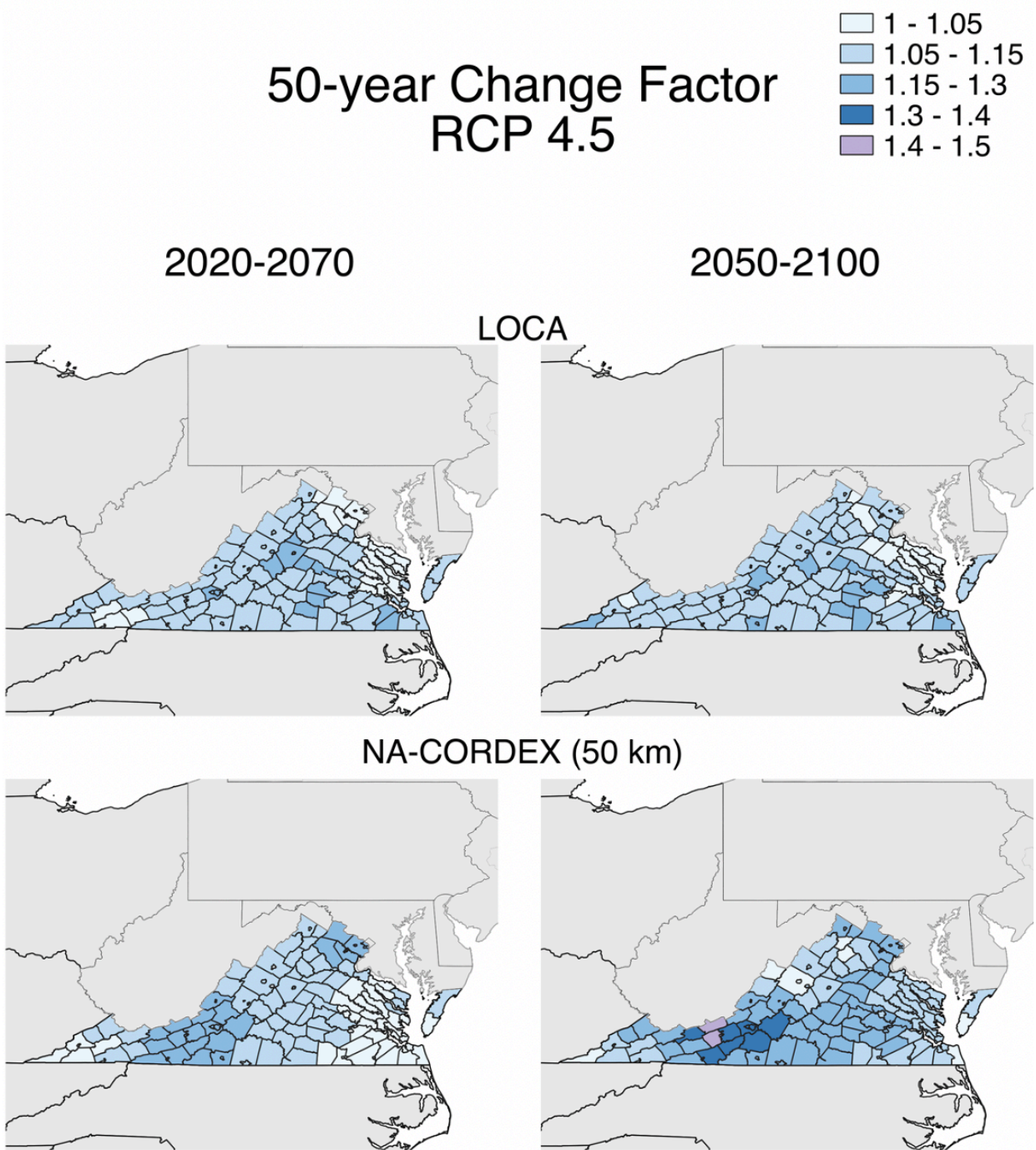
NOTE: This figure represents the time period of 2020–2069 as 2020–2070 and the time period of 2050–2099 as 2050–2100 for ease of understanding.

Figure 5.2. County-Level Change Factors for the CBW Projected by the Ensemble Median of All GCMs in Each Dataset for Both Future Periods Under RCP 8.5



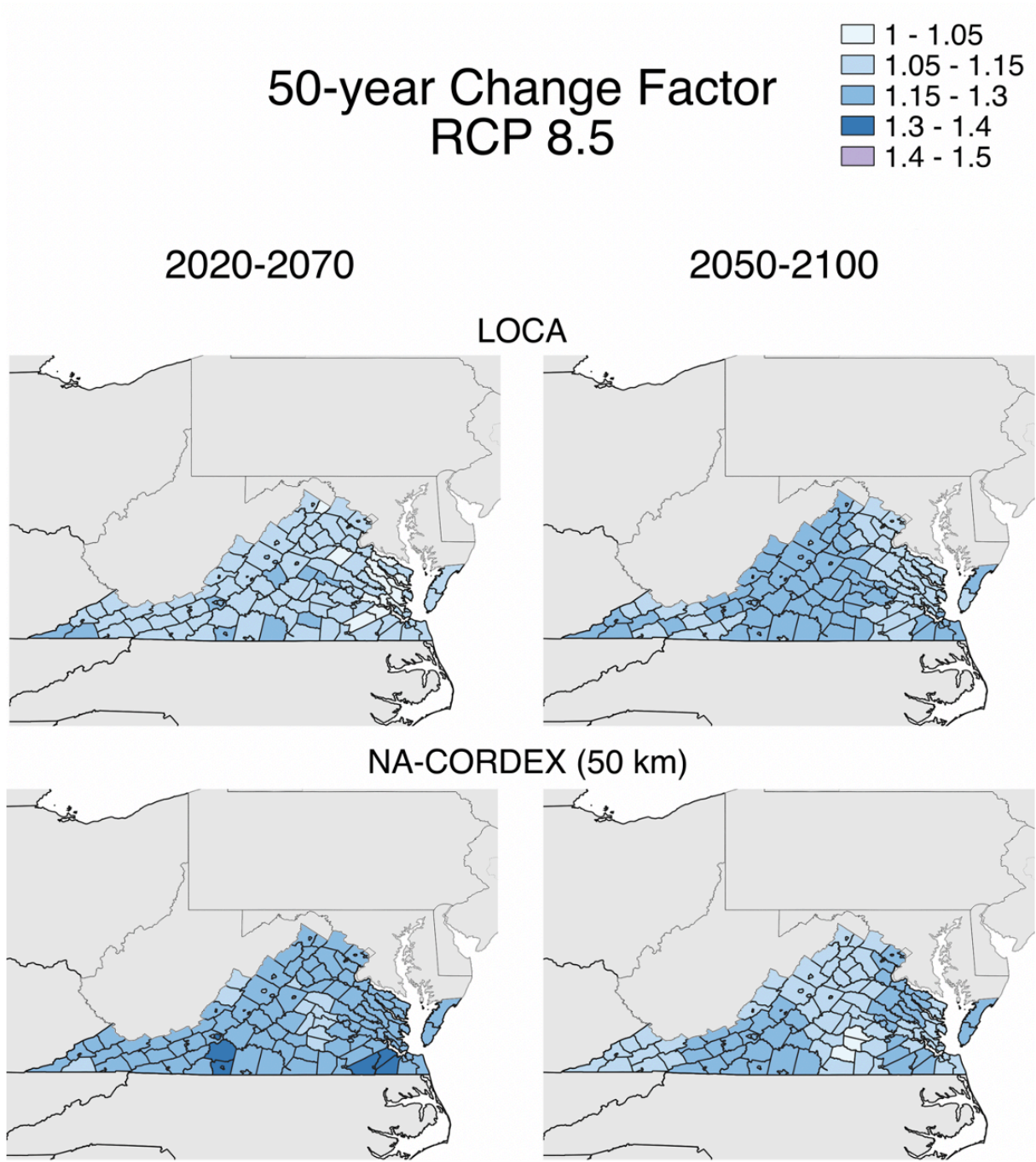
NOTE: This figure represents the time period of 2020–2069 as 2020–2070 and the time period of 2050–2099 as 2050–2100 for ease of understanding.

Figure 5.3. County-Level Change Factors for Virginia Projected by the Ensemble Median of All GCMs in Each Dataset for Both Future Periods Under RCP 4.5



NOTE: This figure represents the time period of 2020–2069 as 2020–2070 and the time period of 2050–2099 as 2050–2100 for ease of understanding.

Figure 5.4. County-Level Change Factors for Virginia Projected by the Ensemble Median of All GCMs in Each Dataset for Both Future Periods Under RCP 8.5

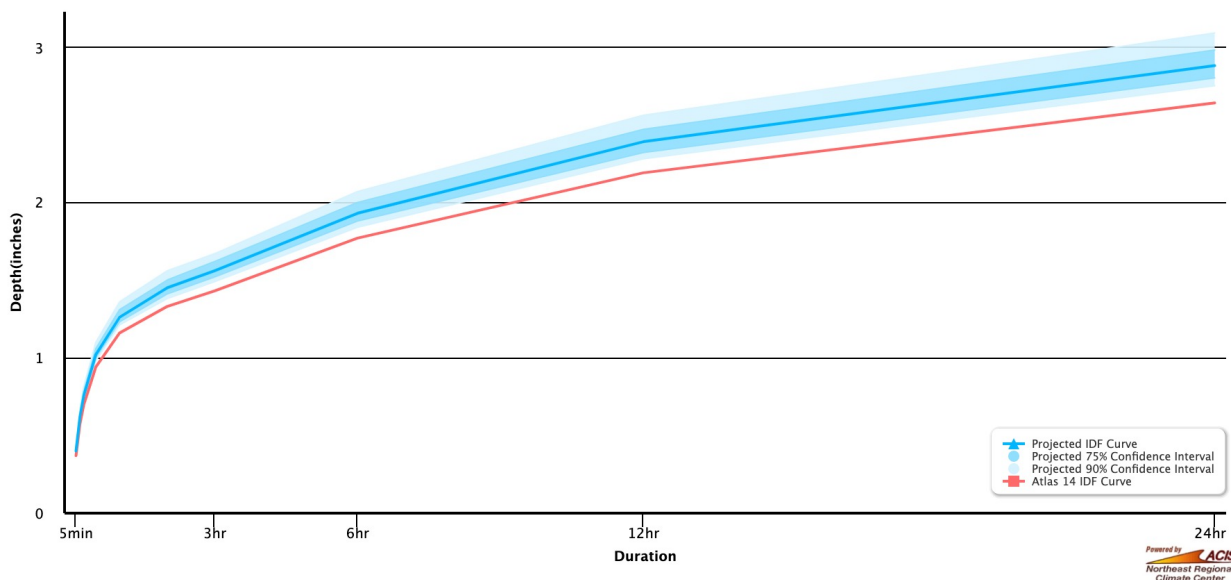


NOTE: This figure represents the time period of 2020–2069 as 2020–2070 and the time period of 2050–2099 as 2050–2100 for ease of understanding.

Accessing IDF Curve Change Factors and Using the Data Tool

The change factors and projected IDF curves are available in an online interactive tool, available at <https://midatlantic-idf.rcc-acis.org>.¹¹³ This tool allows users to search and download the projected station-based IDF curves for five-minute to seven-day durations for the entire CBW and Virginia and county-level IDF curve change factors (described in detail in Chapter 4). Users can select between future time periods (2020–2070 and 2050–2100),¹¹⁴ recurrence intervals (2-, 5-, 10-, 25-, 50-, and 100-year), future greenhouse gas concentration scenarios (RCP 4.5 and 8.5), and the region of interest (CBW or Virginia). All study data are available for download in .csv form (for a station or the entire study region) or graphical form (for IDF curves). A webinar is available under the Technical Resources tab of the online tool that walks through the features and functionality of the tool. Figure 5.5 shows an example projected IDF curve for a two-year recurrence interval from the online tool. The blue solid line indicates the median change factor within the computed uncertainty range, as well as the 75th percentile (blue band) and 90th percentile (light blue band) of the uncertainty range. The red line shows the 1950–2000 Atlas 14 IDF curve for this location and recurrence interval.

Figure 5.5. 2-Year Recurrence Interval IDF Curve for State College, Pennsylvania, Under RCP 4.5 from 2020 Through 2070



¹¹³ Mid-Atlantic Regional Integrated Sciences and Assessments, “Projected Intensity-Duration-Frequency (IDF) Curve Data Tool for the Chesapeake Bay Watershed and Virginia,” undated.

¹¹⁴ The online tool represents the time period 1950–1999 as 1950–2000, 2020–2069 as 2020–2070, and 2050–2099 as 2050–2100 for ease of understanding.

Recommended Application of Change Factors

The online tool offers two types of data: county-level IDF curve change factors and station-based projected IDF curves, which constitute Atlas 14 values with the change factors already applied. To ensure proper use of these two data types, this section highlights recommendations of how and how not to use the IDF curve change factors and adjusted IDF curves. Broadly, we recommend directly using the projected IDF curves available in the online tool for the stations provided. These Atlas 14 stations have been vetted by the study team as being those that include an appropriate historical record, and the research team has already applied future climate change factors to Atlas 14 values. For users who would like to apply change factors to an Atlas 14 IDF curve themselves, we recommend only applying change factors to Atlas 14 IDF curves derived using a similar historical record (1950–2000). In this case, change factors are applied to IDF curve values by multiplying the Atlas 14 depth by the change factor. We do not recommend applying change factors directly to Atlas 14 values that contain a different historical record or that have been updated to include more-recent data. In cases where Atlas 14 has been updated, users could compare the updated Atlas 14 values for a given station to the projected station-based IDF curves for the two future time periods (2020–2070 or 2050–2100) for that same station if it is available in the online tool. These points are summarized below.

Correct applications of the data tool:

- Use the station-based projected Atlas 14 IDF curves in the online tool for typical engineering applications.
- Apply county-level change factors to gridded Atlas 14 values from NOAA’s PFDS within that county and that cover a roughly similar historic period (1950–1999).
- Compare 2020–2070 or 2050–2100 station-based projected Atlas 14 IDF curve values from the tool (not the change factors) with any updated Atlas 14 values that cover a more-recent time period than those offered in the tool.
- Examine the range of uncertainty in the station-based projected Atlas 14 IDF curves or the county-level change factors. For higher-risk sites, consider selecting the 75th- or 90th-percentile value for the IDF curve value as an additional risk mitigation measure.

Incorrect applications of the data tool:

- Apply change factors directly to Atlas 14 values that have a different time period than that in the tool (1950–2000).
- Apply change factors to IDF curves not available from Atlas 14.

6. Summary and Conclusions

The CBW and Virginia have experienced increases in extreme rainfall events over the past decade, exacerbating ongoing stormwater challenges throughout the region.^{115 116} Atlas 14, the dominant source of IDF curves for jurisdictions across the region and the United States, however, uses historic station-based observations and does not incorporate rainfall data observed after 2000 into its IDF curves in the mid-Atlantic region, nor does it consider future precipitation projections. These two key limitations of Atlas 14—the time period used for analysis and assumptions of stationarity—could thus lead to underestimation of precipitation extremes when designing infrastructure for the future. Moreover, the lack of consistent approaches to stormwater management and precipitation data analyses across localities and the willingness of regional planners and engineers to use new tools, particularly updated or projected IDF curves, are motivating factors for this work.¹¹⁷

To this end, the authors of this report developed projected IDF curves that can be easily integrated with existing planning and design methods and used across the CBW and Virginia to plan, design, and build infrastructure assets to be more resilient to climate change. The authors leveraged the best-available science to inform and carry out a transparent, consistent, and straightforward approach to generate IDF curve change factors and apply these factors to Atlas 14 stations. Importantly, the research team incorporated a range of downscaled climate model datasets and future scenarios to reflect the range of plausible changes for IDF curves. Because no single dataset or methodology can fully represent a complex hydrological system, whether historic or projected, this range is critical to consider for planning and design.

To make these results available to a broad regional audience, the research team produced (1) projected IDF curves, based on IDF curve change factors, for two future time periods for the CBW and Virginia and their uncertainty ranges and (2) an interactive online tool that allows end users to navigate these data. This report described the project's data and approach in detail to make the project's methodology clear and transparent to those using the IDF curve tool or those interested in replicating these methods in other contexts.

Of key importance to this work and to climate resilient stormwater management efforts more broadly, the study team developed a transparent, consistent, and straightforward approach to deriving projected IDF curves. From a scientific perspective, transparency is essential to enable

¹¹⁵ Jennifer Runkle, Kenneth E. Kunkel, Laura Stevens, Sarah Champion, Brooke C. Stewart, Rebekah Frankson, and William Sweet, *2017: Virginia State Climate Summary*, NOAA Technical Report NESDIS 149-VA, 2017.

¹¹⁶ Jordan R. Fischbach, Michelle E. Miro, Lauren Kendrick, and Arthur T. DeGaetano, "Chesapeake Bay Watershed Climate Impacts Summary and Outlook for 2018," Mid-Atlantic Regional Integrated Sciences and Assessment, 2018.

¹¹⁷ David Wood and Tom Schueler, *Summary of Stakeholder Concerns, Current Management and Future Needs for Addressing Climate Change Impacts on Stormwater Management*, Chesapeake Stormwater Network, 2020.

the replication of this study's approach as well as facilitate comparison with future research efforts,¹¹⁸ because there is substantial ongoing work to understand the drivers of rainfall extremes in the context of climate change (e.g., advancements in high-resolution convection-permitting climate modeling). Transparency is also of high importance for the application of this study's IDF curves in practice. With clear methodologies drawn from peer-reviewed scientific papers, localities can rely on the robustness of study results or dive into the underlying research to help answer any questions they may have. Finally, this report presents both a consistent and straightforward regional approach to projected IDF curves, which makes results available to all counties within the CBW and Virginia based on the same methodology and data. The application of change factors to adjust widely used Atlas 14 IDF curve values is conceptually straightforward and practical for practitioners across the region.

This consistent approach lends itself to future work updating IDF curves and change factors. The change factors produced in this study should be revisited when CMIP6 is fully released. A routine reexamination of the IDF curves is also warranted as new rainfall observations become available, Atlas 14 is updated, and technical advancements improve IDF curve estimation methods and use. The frequency of these updates should be based on best practices from science, as too-frequent updates could result in IDF curves that fluctuate with interdecadal variability in precipitation. Research is also still needed to inform how the growing historical record of rainfall observations should be used in deriving future IDF curves. Future work should also investigate and validate the application of change factors to sub-hourly durations.

Future work should also focus on communicating and recommending the use of projected IDF curve values in practice. To support an accurate representation of future conditions, this study recommends considering a range of uncertainty in future conditions, shown as the 10th-, 25th-, median, 75th-, and 90th-percentile change factors, posing the question to practitioners of which number to select. Future work should help practitioners answer this question and focus on developing actionable guidance for practitioners and decisionmakers to interpret uncertainty and incorporate a range of future climate projections into planning and decisionmaking, rather than simply selecting the mean or median of climate projections. This type of work is not only applicable to stormwater design but also broadly relevant to climate adaptation projects throughout the United States and across the water sector.

Although future work can enhance this study, given the willingness across the region to use new stormwater management tools, the transparent, consistent, and straightforward set of projected IDF curves produced by this study can serve as a resource for communities to explore anticipated changes across design storms, access future change factors that can be applied to existing design guidelines and mitigate some of the impacts of the region's current and future stormwater management challenges. Furthermore, the application and use of climate-adjusted IDF curves affect community resilience, costs, and impacts. It is critical that policymakers and decisionmakers use transparent and rigorous climate-adjusted IDF curves and explore the

¹¹⁸ Daniel B. Wright, Constantine Samaras, and Tania López-Cantú, "Resilience to Extreme Rainfall Starts with Science," *Bulletin of the American Meteorological Society*, Vol. 102, No. 4, 2021, pp. E808–E813.

implications of uncertainties, especially when these curves support the design of critical infrastructure systems.

References

- Abatzoglou, John T., and Timothy J. Brown, “A Comparison of Statistical Downscaling Methods Suited for Wildfire Applications,” *International Journal of Climatology*, Vol. 32, Vol. 5, April 2012, pp. 772–780.
- Agilan, V., and N. V. Umamahesh, “What Are the Best Covariates for Developing Non-Stationary Rainfall Intensity-Duration-Frequency Relationship?” *Advances in Water Resources*, Vol. 101, March 2017, pp. 11–22.
- Applied Climate Information System, “Datasets,” webpage, 2017. As of June 16, 2021: https://www.rcc-acis.org/docs_datasets.html
- Avery, Christopher W., David R. Reidmiller, Michael Kolian, Kenneth E. Kunkel, David Herring, Reid Sherman, William V. Sweet, Kathryn Tipton, and Christopher P. Weaver, “Data Tools and Scenario Products,” in David R. Reidmiller, Christopher W. Avery, David R. Easterling, Kenneth E. Kunkel, Kristin L. M. Lewis, Thomas K. Maycock, and Brooke C. Stewart, eds., *Impacts, Risks, and Adaptation in the United States: Fourth National Climate Assessment, Volume II*, Washington, D.C.: U.S. Global Change Research Program, 2018, pp. 1413–1430.
- Bonnin, Geoffrey M., Deborah Martin, Bingzhang Lin, Tye Parzybok, Michael Yekta, and David Riley, *NOAA Atlas 14: Precipitation-Frequency Atlas of the United States, Vol. 2, Version 3.0: Delaware, District of Columbia, Illinois, Indiana, Kentucky, Maryland, New Jersey, North Carolina, Ohio, Pennsylvania, South Carolina, Tennessee, Virginia, West Virginia*, Silver Spring, Md.: U.S. Department of Commerce, National Oceanic and Atmospheric Administration, and National Weather Service, 2006. As of June 16, 2021: <https://hdsc.nws.noaa.gov/hdsc/pfds/docs/NA14Vol2.pdf>
- Butcher, Jonathan B., Tan Zi, Brian R. Pickard, Scott C. Job, Thomas E. Johnson, and Bryan A. Groza, “Efficient Statistical Approach to Develop Intensity-Duration-Frequency Curves for Precipitation and Runoff Under Future Climate,” *Climatic Change*, Vol. 164, No. 1, 2021, pp. 1–20.
- Cannon, Alex J., Stephen R. Sobie, and Trevor Q. Murdock, “Bias Correction of GCM Precipitation by Quantile Mapping: How Well Do Methods Preserve Changes in Quantiles and Extremes?” *Journal of Climate*, Vol. 28, No. 17, 2015, pp. 6938–6959.
- Charochak, Michelle, and James Bass, *Preparing for Increases in Extreme Precipitation Events in Local Planning and Policy on Maryland’s Eastern Shore*, a report prepared for the Eastern Shore Climate Adaptation Partnership by Eastern Shore Land Conservancy, January 2020. As of June 16, 2021: <https://www.eslc.org/wp-content/uploads/2020/01/ExtremePrecipitationReport.pdf>

- Cheng, Linyin, and Amir AghaKouchak, “Nonstationary Precipitation Intensity-Duration-Frequency Curves for Infrastructure Design in a Changing Climate,” *Scientific Reports*, Vol. 4, November 2014.
- Chesapeake Bay Foundation, “Geography and Facts,” webpage, undated. As of March 30, 2021: <https://www.cbf.org/about-the-bay/chesapeake-bay-watershed-geography-and-facts.html>
- Chesapeake Bay Foundation, “The Chesapeake Bay Watershed,” January 24, 2008. As of July 6, 2021: <https://www.cbf.org/about-the-bay/maps/geography/chesapeake-bay-watershed.html>
- Chesapeake Bay Program, “Urban Stormwater Workgroup,” webpage, undated. As of March 30, 2021: https://www.chesapeakebay.net/who/group/urban_stormwater_workgroup
- Cook, Lauren M., Christopher J. Anderson, and Constantine Samaras, “Framework for Incorporating Downscaled Climate Output into Existing Engineering Methods: Application to Precipitation Frequency Curves,” *Journal of Infrastructure Systems*, Vol. 23, No. 4, December 2017.
- Cook, Lauren M., Seth McGinnis, and Constantine Samaras, “The Effect of Modeling Choices on Updating Intensity-Duration-Frequency Curves and Stormwater Infrastructure Designs for Climate Change,” *Climatic Change*, Vol. 159, No. 2, 2020, pp. 289–308.
- Data.gov, “Integrated Surface Global Hourly Data,” National Climatic Data Center, 2021. As of June 16, 2021: <https://catalog.data.gov/dataset/integrated-surface-global-hourly-data>
- DeGaetano, Arthur T., and Christopher M. Castellano, “Future Projections of Extreme Precipitation Intensity-Duration-Frequency Curves for Climate Adaptation Planning in New York State,” *Climate Services*, Vol. 5, January 2017, pp. 23–35.
- DeGaetano, Arthur T., and Christopher Castellano, “Selecting Time Series Length to Moderate the Impact of Nonstationarity in Extreme Rainfall Analyses,” *Journal of Applied Meteorology and Climatology*, Vol. 57, No. 10, 2018, pp. 2285–2296.
- Eyring, Veronika, Sandrine Bony, Gerald A. Meehl, Catherine A. Senior, Bjorn Stevens, Ronald J. Stouffer, and Karl E. Taylor, “Overview of the Coupled Model Intercomparison Project Phase 6 (CMIP6) Experimental Design and Organization,” *Geoscientific Model Development*, Vol. 9, 2016, pp. 1937–1958.
- Fischbach, Jordan R., Michelle E. Miro, Lauren Kendrick, and Arthur T. DeGaetano, “Chesapeake Bay Watershed Climate Impacts Summary and Outlook for 2018,” Mid-Atlantic Regional Integrated Sciences and Assessment, 2018. As of June 16, 2021: <https://www.midatlanticrisa.org/climate-summaries/2018/11.html>

- Fischbach, Jordan R., Michelle E. Miro, Krista Romita Grocholski, Arthur T. DeGaetano, and Samantha Borisoff, “Chesapeake Bay Watershed Climate Impacts Summary and Outlook: Winter 2018–2019,” Mid-Atlantic Regional Integrated Sciences and Assessment, 2019. As of June 16, 2021:
<https://www.midatlanticrisa.org/climate-summaries/2019/03.html>
- Fowler, Hayley J., Haider Ali, Richard P. Allan, Nikolina Ban, Renaud Barbero, Peter Berg, Stephen Blenkinsop, Nalan Senol Cabi, Steven Chan, Murray Dale, Robert J. H. Dunn, Marie Ekström, Jason P. Evans, Giorgia Fosser, Brian Golding, Selma B. Guerreiro, Gabriele C. Hegerl, Abdullah Kahraman, Elizabeth J. Kendon, Geert Lenderink, Elizabeth Lewis, Xiaofeng Li, Paul A. O’Gorman, Harriet G. Orr, Katy L. Peat, Andreas F. Prein, David Pritchard, Christoph Schär, Ashish Sharma, Peter A. Stott, Roberto Villalobos-Herrera, Gabriele Villarini, Conrad Wasko, Michael F. Wehner, Seth Westra, and Anna Whitford, “Towards Advancing Scientific Knowledge of Climate Change Impacts on Short-Duration Rainfall Extremes,” *Philosophical Transactions of the Royal Society A: Mathematical, Physical and Engineering Sciences*, Vol. 379, No. 2195, April 2021.
- Gilleland, Eric, and Richard W. Katz, “extRemes 2.0: An Extreme Value Analysis Package in R,” *Journal of Statistical Software*, Vol. 72, No. 8, 2016, pp. 1–39.
- Helsel, Dennis R., Robert M. Hirsch, Karen R. Ryberg, Stacey A. Archfield, and Edward J. Gilroy, *Statistical Methods in Water Resources: U.S. Geological Survey Techniques and Methods*, Book 4, Chapter A3, Reston, Va.: U.S. Geological Survey, 2020.
- Hosking, J. R. M., “L-Moments: Analysis and Estimation of Distributions Using Linear Combinations of Order Statistics,” *Journal of the Royal Statistical Society, Series B (Methodological)*, Vol. 52, No. 1, 1990, pp. 105–124.
- Kharin, Viatcheslav V., and Francis W. Zwiers, “Changes in the Extremes in an Ensemble of Transient Climate Simulations with a Coupled Atmosphere–Ocean GCM,” *Journal of Climate*, Vol. 13, No. 21, 2000, pp. 3760–3788.
- Kim, Hanbeen, Sooyoung Kim, Hongjoon Shin, and Jun-Haeng Heo, “Appropriate Model Selection Methods for Nonstationary Generalized Extreme Value Models,” *Journal of Hydrology*, Vol. 547, April 2017, pp. 557–574.
- Kuo, Chun-Chao, Thian Yew Gan, and Mesgana Seyoum, “Potential Impact of Climate Change on Intensity Duration Frequency Curves of Central Alberta,” *Climatic Change*, Vol. 130, No. 2, 2015, pp. 115–129.
- Lawrence Livermore National Laboratory, “Program for Climate Model Diagnosis and Intercomparison,” webpage, 2021. As of June 16, 2021:
<https://pcmdi.llnl.gov/mips/cmip5/index.html>

- López-Cantú, Tania, Andreas F. Prein, and Constantine Samaras, “Uncertainties in Future U.S. Extreme Precipitation from Downscaled Climate Projections,” *Geophysical Research Letters*, Vol. 47, No. 9, May 16, 2020.
- Maraun, D., F. Wetterhall, A. M. Ireson, R. E. Chandler, E. J. Kendon, M. Widmann, S. Brienen, H. W. Rust, T. Sauter, M. Themeßl, V. K. C. Venema, K. P. Chun, C. M. Goodess, R. G. Jones, C. Onof, M. Vrac, and I. Thiele-Eich, “Precipitation Downscaling Under Climate Change: Recent Developments to Bridge the Gap Between Dynamical Models and the End User,” *Reviews of Geophysics*, Vol. 48, No. 3, September 2010.
- Martins, Eduardo S., and Jerry R. Stedinger, “Generalized Maximum-Likelihood Generalized Extreme-Value Quantile Estimators for Hydrologic Data,” *Water Resources Research*, Vol. 36, No. 3, March 2000, pp. 737–744.
- Mearns, L. O., et al., *The NA-CORDEX Dataset*, Version 1.0, Boulder Colo.: NCAR Climate Data Gateway, 2017. As of June 16, 2021:
<https://na-cordex.org>
- Mid-Atlantic Regional Integrated Sciences and Assessments, “Projected Intensity-Duration-Frequency (IDF) Curve Data Tool for the Chesapeake Bay Watershed and Virginia,” undated. As of June 16, 2021:
<https://midatlantic-idf.rcc-acis.org>
- Milly, P. C. D., Julio Betancourt, Malin Falkenmark, Robert M. Hirsch, Zbigniew W. Kundzewicz, Dennis P. Lettenmaier, and Ronald J. Stouffer, “Stationarity Is Dead: Whither Water Management?” *Science*, Vol. 319, No. 5863, February 1, 2008, pp. 573–574.
- Miro, Michelle E., Krista Romita Grocholski, Samantha Borisoff, Jordan R. Fischbach, and Arthur T. DeGaetano, “Chesapeake Bay Watershed Climate Impacts Summary and Outlook: Summer 2019,” Mid-Atlantic Regional Integrated Sciences and Assessments, 2019. As of June 16, 2021:
<https://www.midatlanticrisa.org/climate-summaries/2019/09.html#fnref12>
- National Weather Service, “Cooperative Observer Program (COOP),” webpage, undated. As of June 16, 2021:
<https://www.weather.gov/coop/overview>
- Niemczynowicz, Janusz, “Impact of the Greenhouse Effect on Sewerage Systems—Lund Case Study,” *Hydrological Sciences Journal*, Vol. 34, No. 6, 1989, pp. 651–666.
- NOAA National Centers for Environmental Information, “Hourly Precipitation Data,” webpage, undated. As of June 16, 2021:
<https://www.ncdc.noaa.gov/IPS/hpd/hpd.html>
- Olsson, J., K. Berggren, M. Olofsson, and M. Viklander, “Applying Climate Model Precipitation Scenarios for Urban Hydrological Assessment: A Case Study in Kalmar City, Sweden,”

- Atmospheric Research*, 7th International Workshop on Precipitation in Urban Areas, Vol. 92, No. 3, May 2009, pp. 364–375.
- Papalexiou, Simon M., and Demetris Koutsoyiannis, “Battle of Extreme Value Distributions: A Global Survey on Extreme Daily Rainfall,” *Water Resources Research*, Vol. 49, No. 1, January 2013, pp. 187–201.
- Parsons, Jim, “Virginia Beach Makes Plans to Keep Its Head Above Water,” *Engineering News Record*, April 28, 2019. As of June 16, 2021:
<https://www.enr.com/articles/47421-virginia-beach-makes-plans-to-keep-its-head-above-water>
- Perica, Sanja, Sandra Pavlovic, Michael St. Laurent, Carl Trypaluk, Dale Unruh, Deborah Martin, and Orlan Wilhite, *NOAA Atlas 14: Precipitation-Frequency Atlas of the United States, Vol. 10, Version 3.0, Northern States: Connecticut, Maine, Massachusetts, New Hampshire, New York, Rhode Island, Vermont*, Silver Spring, Md.: U.S. Department of Commerce, National Oceanic and Atmospheric Administration, and National Weather Service, 2019. As of June 16, 2021:
https://www.weather.gov/media/owp/oh/hdsc/docs/Atlas14_Volume10.pdf
- Pierce, David W., Daniel R. Cayan, and Bridget L. Thrasher, “Statistical Downscaling Using Localized Constructed Analogs (LOCA),” *Journal of Hydrometeorology*, Vol. 15, No. 6, 2014, pp. 2558–2585.
- Poschlod, Benjamin, Ralf Ludwig, and Jana Sillmann, “Ten-Year Return Levels of Sub-Daily Extreme Precipitation over Europe,” *Earth System Science Data*, Vol. 13, No. 3, 2021, pp. 983–1003.
- Python, “lmoments 0.2.3,” webpage, February 17, 2015. As of June 16, 2021:
<https://pypi.org/project/lmoments/>
- Ragno, Elisa, Amir AghaKouchak, Charlotte A. Love, Linyin Cheng, Farshid Vahedifard, and Carlos H. R. Lima, “Quantifying Changes in Future Intensity-Duration-Frequency Curves Using Multimodel Ensemble Simulations,” *Water Resources Research*, Vol. 54, No. 3, 2018, pp. 1751–1764.
- Riahi, Keywan, Shilpa Rao, Volker Krey, Cheolhung Cho, Vadim Chirkov, Guenther Fischer, Georg Kindermann, Nebojsa Nakicenovic, and Peter Rafaj, “RCP 8.5—A Scenario of Comparatively High Greenhouse Gas Emissions,” *Climatic Change*, Vol. 109, No. 33, 2011.
- Runkle, Jennifer, Kenneth E. Kunkel, Laura Stevens, Sarah Champion, Brooke C. Stewart, Rebekah Frankson, and William Sweet, *2017: Virginia State Climate Summary*, NOAA Technical Report NESDIS 149-VA, 2017.
- Sarhadi, Ali, and Eric D. Soulis, “Time-Varying Extreme Rainfall Intensity-Duration-Frequency Curves in a Changing Climate,” *Geophysical Research Letters*, Vol. 44, No. 5, March 16, 2017, pp. 2454–2463.

- Segond, M.-L., C. Onof, and H. S. Wheater, “Spatial–Temporal Disaggregation of Daily Rainfall from a Generalized Linear Model,” *Journal of Hydrology*, Vol. 331, Nos. 3–4, December 2006, pp. 674–689.
- Shin, Hongjoon, Younghun Jung, Changsam Jeong, and Jun-Haeng Heo, “Assessment of Modified Anderson–Darling Test Statistics for the Generalized Extreme Value and Generalized Logistic Distributions,” *Stochastic Environmental Research and Risk Assessment*, Vol. 26, No. 1, 2012, pp. 105–114.
- Smirnov, Dmitry, Jason Giovannettone, Seth Lawler, Mathini Sreetharan, Joel Plummer, Brad Workman, and Brian Batten, *Analysis of Historical and Future Heavy Precipitation, City of Virginia Beach, Virginia*, Virginia Beach, Va.: Department of Public Works, 2018. As of June 16, 2021:
<https://www.vbgov.com/government/departments/public-works/storm-water/Documents/SW%20Master%20Planning/anaylsis-hist-and-future-hvy-precip-4-2-18.pdf>
- Srivastav, Roshan K., Andre Schardong, and Slobodan P. Simonovic, “Equidistance Quantile Matching Method for Updating IDF Curves Under Climate Change,” *Water Resources Management*, Vol. 28, No. 9, 2014, pp. 2539–2562.
- Switzman, Harris, Tara Razavi, Serge Traore, Paulin Coulibaly, Donald H. Burn, John Henderson, Edmundo Fausto, and Ryan Ness, “Variability of Future Extreme Rainfall Statistics: Comparison of Multiple IDF Projections,” *Journal of Hydrologic Engineering*, Vol. 22, No. 10, October 2017.
- Taylor, Karl E., Ronald J. Stouffer, Gerald A. Meehl, “An Overview of CMIP5 and the Experiment Design,” *Bulletin of the American Meteorological Society*, Vol. 93, No. 4, 2012, pp. 485–498.
- Te Chow, V., D. R. Maidment, and L. W. Mays, “Applied Hydrology,” *Journal of Engineering Education*, Vol. 308, 1962, p. 1959.
- Teutschbein, Claudia, and Jan Seibert, “Bias Correction of Regional Climate Model Simulations for Hydrological Climate-Change Impact Studies: Review and Evaluation of Different Methods,” *Journal of Hydrology*, Vol. 456–457, August 16, 2012, pp. 12–29.
- Thakali, Ranjeet, Ajay Kalra, and Sajjad Ahmad, “Understanding the Effects of Climate Change on Urban Stormwater Infrastructures in the Las Vegas Valley,” *Hydrology*, Vol. 3, No. 4, 2016, p. 34.
- Thomson, Allison M., Katherine V. Calvin, Steven J. Smith, G. Page Kyle, April Volke, Pralit Patel, Sabrina Delgado-Arias, Ben Bond-Lamberty, Marshall A. Wise, Leon E. Clarke, and James A. Edmonds, “RCP4.5: A Pathway for Stabilization of Radiative Forcing by 2100,” *Climatic Change*, Vol. 109, No. 77, 2011.

- Wilby, R. L., and T. M. Wigley, “Downscaling General Circulation Model Output: A Review of Methods and Limitations,” *Progress in Physical Geography*, Vol. 21, No. 4, 1997, pp. 530–548.
- Wood, David, *Review of Current Stormwater Engineering Standards and Criteria for Rainfall and Runoff Modeling in the Chesapeake Bay Watershed*, Chesapeake Stormwater Network, 2020. As of June 16, 2021:
https://chesapeakestormwater.net/wp-content/uploads/dlm_uploads/2020/10/Memo-2_Stormwater-Standards_FINAL_10.20.20-1.pdf
- Wood, David, and Tom Schueler, *Summary of Stakeholder Concerns, Current Management and Future Needs for Addressing Climate Change Impacts on Stormwater Management*, Chesapeake Stormwater Network, 2020. As of June 16, 2021:
https://chesapeakestormwater.net/wp-content/uploads/dlm_uploads/2020/02/FINAL-Climate-Change-and-Stormwater-Survey-Memo.pdf
- World Climate Research Program Working Group on Coupled Modeling, *CMIP6—Coupled Model Intercomparison Project Phase 6*, Livermore, Calif.: Lawrence Livermore National Laboratory, 2021. As of June 16, 2021:
<https://pcmdi.llnl.gov/CMIP6>
- Wright, Daniel B., Constantine Samaras, and Tania López-Cantú, “Resilience to Extreme Rainfall Starts with Science,” *Bulletin of the American Meteorological Society*, Vol. 102, No. 4, 2021, pp. E808–E813.
- Wu, Shu, Momcilo Markus, David Lorenz, James R. Angel, and Kevin Grady, “A Comparative Analysis of the Historical Accuracy of the Point Precipitation Frequency Estimates of Four Data Sets and Their Projections for the Northeastern United States,” *Water*, Vol. 11, No. 6, 2019, p. 1279.
- Wuertz, David, Jay Lawrimore, and Bryant Korzeniewski, *Cooperative Observer Program (COOP) Hourly Precipitation Data (HPD)*, Version 2.0, NOAA National Centers for Environmental Information, 2018.
- van Vuuren, Detlef P., Jae Edmonds, Mikiko Kainuma, Keywan Riahi, Allison Thomson, Kathy Hibbard, George C. Hurtt, Tom Kram, Volker Krey, Jean-Francois Lamarque, Toshihiko Masui, Malte Meinshausen, Nebojsa Nakicenovic, Steven J. Smith, and Steven K. Rose, “The Representative Concentration Pathways: An Overview,” *Climatic Change*, Vol. 109, No. 5, 2011.